GEORGIA INSTITUTE OF TECHNOLOGY — OFFICE OF CONTRACT ADMINISTRATION

PROJECT ADMINISTRATION DATA SHEET

[x] ORIGINAL [ ] REVISION NO. _____

Project No. A-3253 — DATE 6/1/82

Project Director: E. A. Nelson CO — School/Lab RAIL/RAD

Sponsor: Bendix Avionics Division, Ft. Lauderdale, FL.

Type Agreement: Purchase Order No. N90749

Award Period: From 4/21/82 To 7/16/82 (Performance) _____ (Reports)

Sponsor Amount: $10,000 — Contracted through:

Cost Sharing: None — GTRI/GTRC

Title: Helicopter Radar Study

ADMINISTRATIVE DATA

OCA Contact William F. Brown x 4820

1) Sponsor Technical Contact:

Mr. Ross Norsworthy
The Bendix Corp.
Avionics Div.
2100 Northwest 62nd St.
P. O. Box 9414
Ft. Lauderdale, FL 33310

2) Sponsor Admin/Contractual Matters:

Ms. Jackie B. Rule, Buyer
The Bendix Corp.
Avionics Div.
2100Northwest62nd St.
P. O. Box 9414
Ft, Lauderdale, FL 33310
(305) 776-4100

Defense Priority Rating: none

Security Classification: none

RESTRICTIONS

See Attached _____ Supplemental Information Sheet for Additional Requirements.

Travel: Foreign travel must have prior approval – Contact OCA in each case. Domestic travel requires sponsor approval where total will exceed greater of $500 or 125% of approved proposal budget category.

Equipment: Title vests with none proposed or anticipated

COMMENTS:

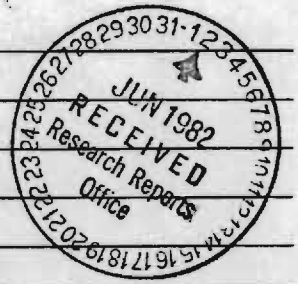

COPIES TO:

Administrative Coordinator
Research Property Management
Accounting
Procurement/EES Supply Services
Research Security Services
Reports Coordinator (OCA)
Legal Services (OCA)
Library
EES Public Relations (2)
Computer Input
Project File
Other _____

FORM OCA 4:781

GEORGIA INSTITUTE OF TECHNOLOGY OFFICE OF CONTRACT ADMINISTRATION

SPONSORED PROJECT TERMINATION SHEET

Date 10/18/82

Project Title: Helicopter Radar Study

Project No: A-3253

Project Director: E. A. Nelson

Sponsor: Bendix Avionics Division, Ft. Lauderdale, FL.

Effective Termination Date: 7/16/82

Clearance of Accounting Charges: 7/16/82

Grant/Contract Closeout Actions Remaining:

- [x] Final Invoice and Closing Documents
- [ ] Final Fiscal Report
- [ ] Final Report of Inventions
- [ ] Govt. Property Inventory & Related Certificate
- [ ] Classified Material Certificate
- [ ] Other _____

Assigned to: RAIL/AD (School/Laboratory)

COPIES TO:

Administrative Coordinator	Research Security Services	EES Public Relations (2)
Research Property Management	Reports Coordinator (OCA)	Computer Input
Accounting	Legal Services (OCA)	Project File
Procurement/EES Supply Services	Library	Other _____

FORM OCA 10-781

A-3253

FINAL TECHNICAL REPORT

GIT/EES Project A-3253

HELICOPTER ALL-WEATHER LANDING SYSTEM
ROTARY-WING ANTENNA STUDY

September 1982

E. A. Nelson and P. P. Britt

Prepared for

THE BENDIX CORPORATION

AVIONICS DIVISION

Fort Lauderdale, FL 33310

Under Purchase Order Number N90749

Prepared by

GEORGIA INSTITUTE OF TECHNOLOGY

A Unit of the University System of Georgia

ENGINEERING EXPERIMENT STATION

Atlanta, Georgia 30332

TABLE OF CONTENTS

LIST OF ILLUSTRATIONS

LIST OF ILLUSTRATIONS (cont.)

LIST OF TABLES

LIST OF TABLES

SECTION 1
INTRODUCTION

The Engineering Experiment Station at the Georgia Institute of Technology conducted a study of an X-band rotary wing antenna and a dual frequency (X-band and millimeter wave) forward looking radar.

The primary technical considerations for the antenna were: (1) elevation directivity and front-to-back ratio and (2) compatibility with rotary wing structure. Edge slotted and broadwall slotted waveguide concepts for the rotary wing X-band antenna were investigated using computer modeling techniques. None of the edge slotted waveguide antenna concepts investigated provided acceptable elevation patterns. Several broadwall slotted waveguide antenna concepts investigated yielded elevation patterns that could be acceptable. Details of this investigation are included in Section 2.

The dual frequency radar investigation included an analysis of millimeter wave radar performance, a hybrid dual frequency antenna, and a parabolic dual frequency antenna. The analysis of millimeter wave radar performance included consideration of angular resolution, weather losses, weather clutter, signal margin, and mapping sensitivity. For the scenario investigated, a 95-GHz radar operating in rain as heavy as 25 mm/hr will not detect smooth terrain until the range closes to less than about 200 meters. The 95-GHz radar could be used to look for corner reflectors or other scatterers that must be avoided; if nothing is visible, the area can be assumed to be clear of obstacles. The hybrid antenna investigated was a 9.6-GHz slot array combined with a 95-GHz feed, a dichroic parabolic transflector, and a dichroic polarization twist mirror. The parabolic antenna investigated was a dual frequency feed, a parabolic transflector, a dichroic polarization twist mirror, and a 9.5-GHz polarization twist reflector. Details of this investigation are included in Section 3.

SECTION 2
ROTARY WING X-BAND ANTENNA

2.1 OVERVIEW

The rotary wing for a helicopter can provide a location for an antenna that will permit high azimuth resolution surface mapping. The antenna must be integrable with present wing designs without compromising wing performance. A slotted waveguide can easily be inserted into the wing as illustrated in Figure 1. A small cross section of the nomex core is removed and replaced by the waveguide. There is little or no increase in weight and no loss of strength or flexibility. The required frequency, impedance, and azimuth pattern performance are also easily achieved with a slotted waveguide antenna.

The elevation patterns of the basic slotted waveguide line sources, however, are very broad with very high back radiation. An azimuth pattern at a constant elevation angle indicates relative pattern levels at the corresponding constant range. Because of the large azimuth aperture, the azimuth patterns will appear as a narrow main beam and a narrow back lobe at $\pm 180^{o}$. The ratio of the main beam to back lobe level for any constant elevation (constant range) is then the front-to-back ratio for that range.

The criteria for desired elevation pattern performance is the ability to distinguish an object near the surface from one in the opposite direction, but at the same range, as shown in Figure 2. An estimated front-to-back ratio of 20 dB is needed; without this antenna directional capability, a more expensive range/Doppler radar would be required.

Antenna configurations considered were based on edge slotted and broadwall slotted waveguides. Computer modeling techniques were used to evaluate antenna concepts to determine whether the desired elevation pattern could be obtained by a configuration that is compatible with present helicopter wing designs. Edge slotted waveguide antenna concepts investigated did not provide acceptable elevation patterns. Several configurations of broadwall slotted waveguide antenna concepts yielded elevation patterns that could be acceptable. The study results indicate that sufficient control of the antenna elevation pattern can be obtained with an antenna that is relatively simple in cross section and compatible with basic helicopter wing designs.

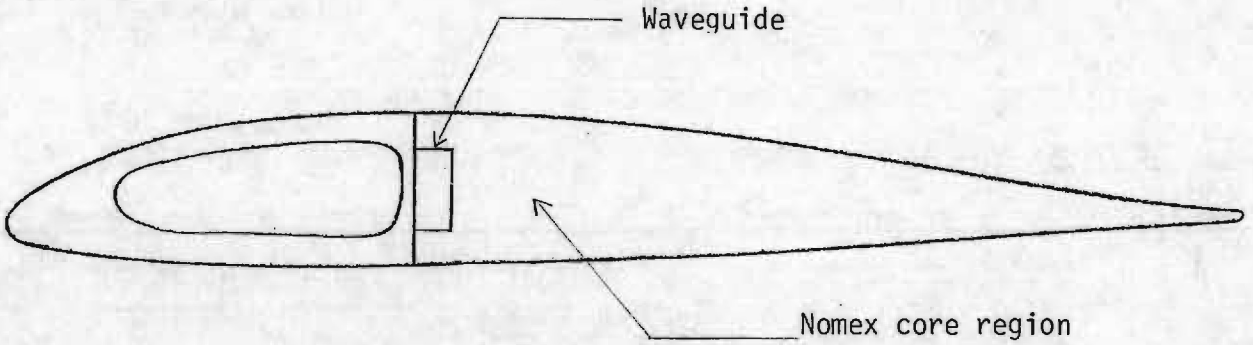

Figure 1. Slotted waveguide antenna in helicopter wing.

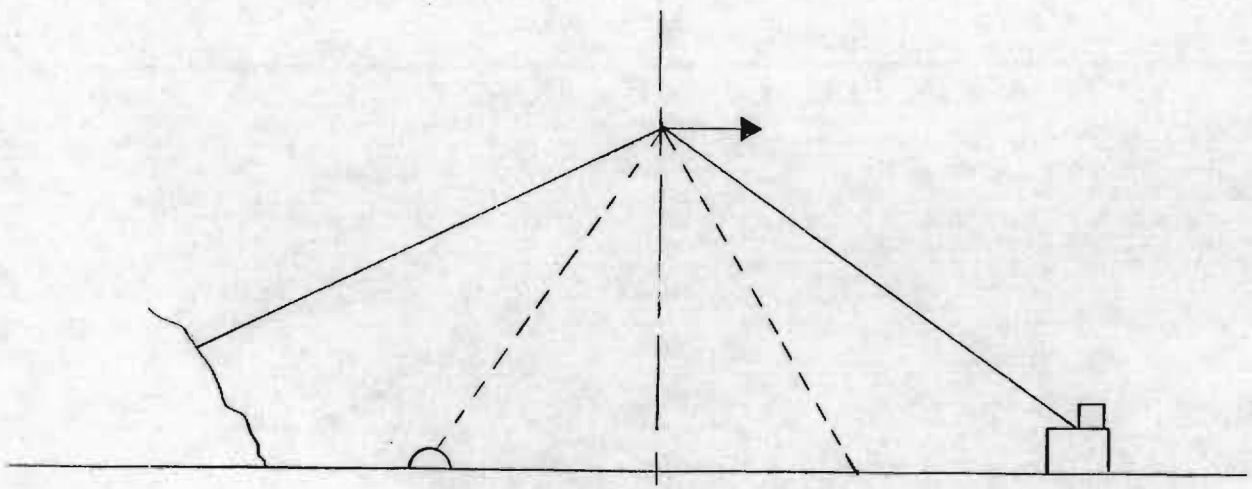

Figure 2. Forward-aft discrimination.

2.2 APPROACH

Antenna concepts formulated in this study were evaluated by a method-of-moments computer analysis based on Rumsey's reactance integral equation.[1,2] The computer program can analyze radiating or scattering structures that can be built up with wires or conducting flat rectangular plates. Currents on the structures, far field patterns, and impedances can be obtained. Figure 3 illustrates how the structure is segmented into dipole modes. More detail in modeling and a greater number of modes per unit area are required to obtain accurate impedances than are required for accurate far field patterns. Far field radiation patterns were the concern of this study.

Antenna configurations considered were based on edge slotted and broadwall slotted waveguides. The elevation patterns for the basic line sources are shown in Figures 4 and 5. In either case, the patterns are very broad with high levels of back radiation. Various arrangements of horns (reflecting plates) and wire directors were used to control the elevation pattern. The criteria for trial configurations were simplicity and wing design compatibility.

A capacitively loaded loop was used as a model for a slot to minimize computer costs. An infinitesimal loop is, of course, the exact dual of an infinitesimal slot in a ground plane. By capacitive loading, a finite loop can be made to have radiation characteristics much like those of a slot. Figures 6, 7, and 8 show some comparisons of patterns for a cavity backed half wavelength slot and a half wavelength loop when both are on a one wavelength square ground plane. For the structures examined, the detailed nature of the slot model was more than overshadowed by the rest of the structure.

2.3 EDGE SLOTTED WAVEGUIDE ANTENNA

Edge slotted waveguide antenna configurations investigated did not provide acceptable elevation patterns, although they did show some improvment over the basic line source pattern (Figure 4). Figure 9 shows the results of using a choke in an attempt to reduce current flow to the back of the waveguide. A 10 dB reduction in gain was achieved directly to the rear, but this approach did not appear to offer much success. Figure 10 shows the pattern achieved with a horn of the trough type frequently used with edge

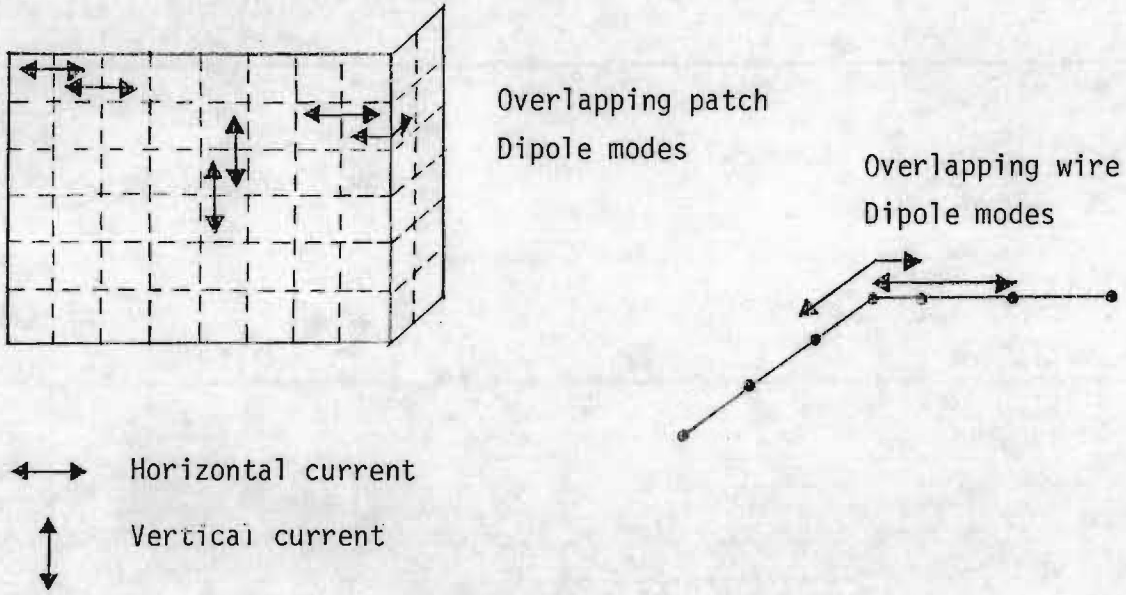

o Segments are usually less than λ/4

Figure 3. Plate and wire mode segments.

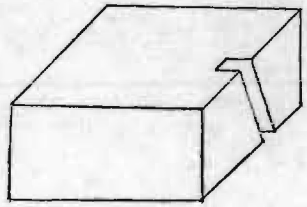

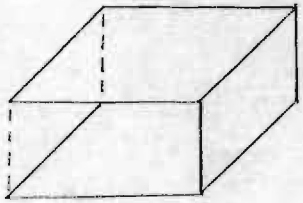

- o Plates with dotted edges not included in model
- o See Figure 6 for slot model

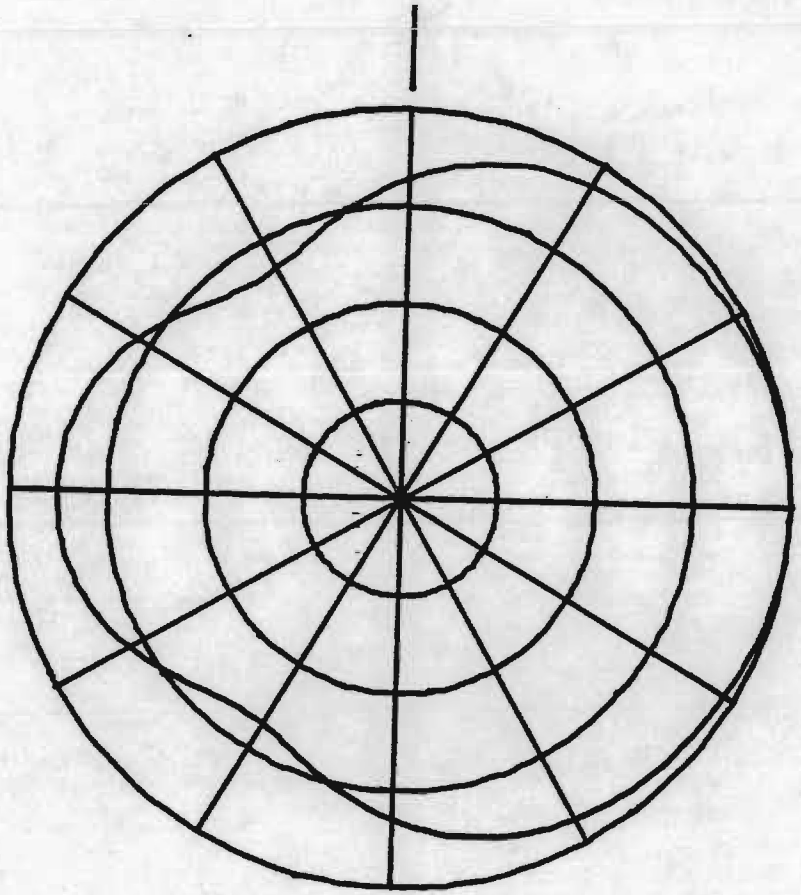

Figure 4. Edge slotted waveguide elevation pattern.

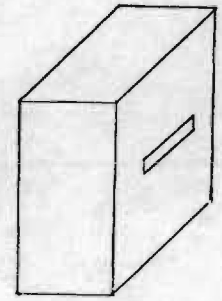

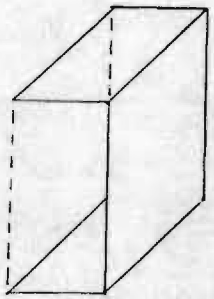

- o Plate with dotted edges not in model
- o See Figure 6 for slot model

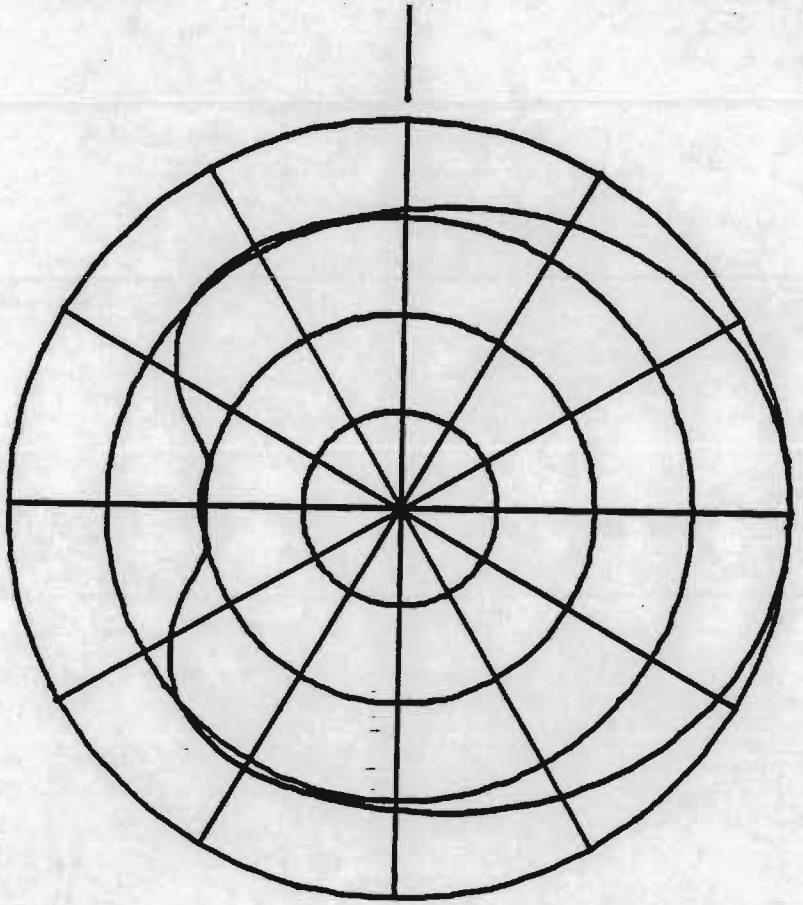

Figure 5. Broadwall slotted waveguide elevation pattern.

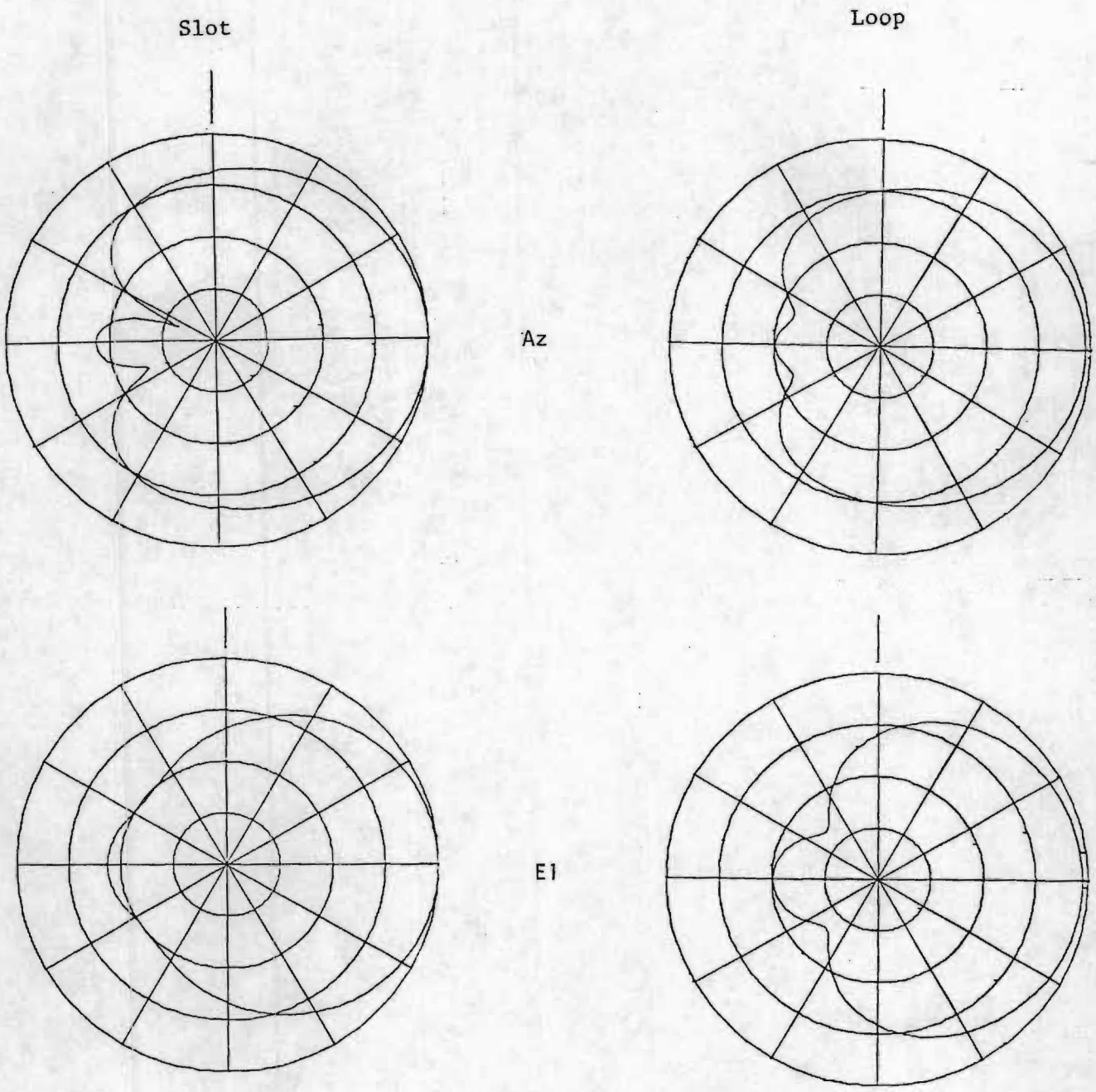

- Major Plane Patterns
- 10 dB/div.
- No significant vertical polarizations in these plans

Figure 6. Loop - Slot Comparison

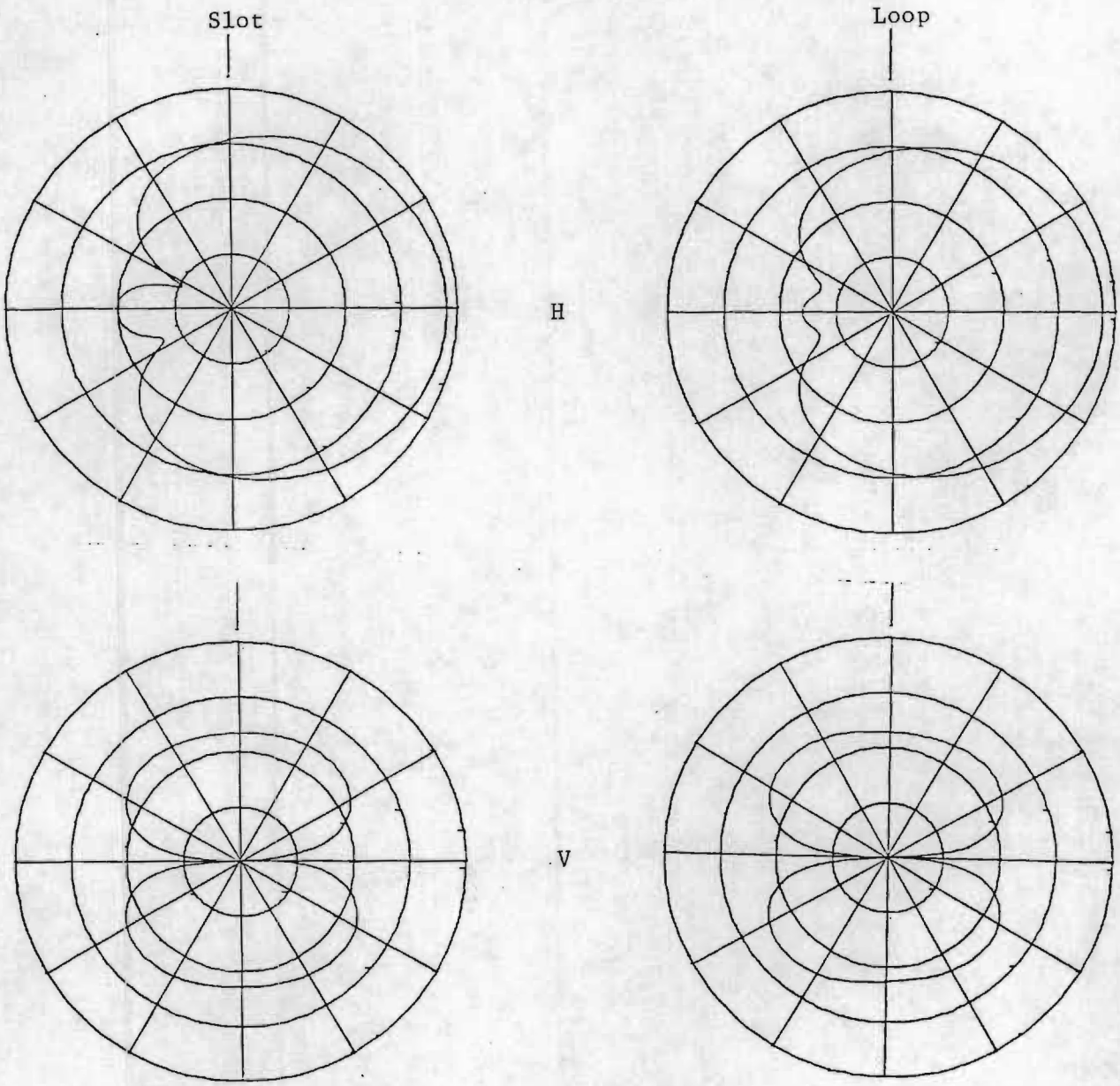

- 30^{o} elevation plane
- 10 dB/div.
- Hor & Vert. Pol.

Figure 7. Loop - Slot Comparison

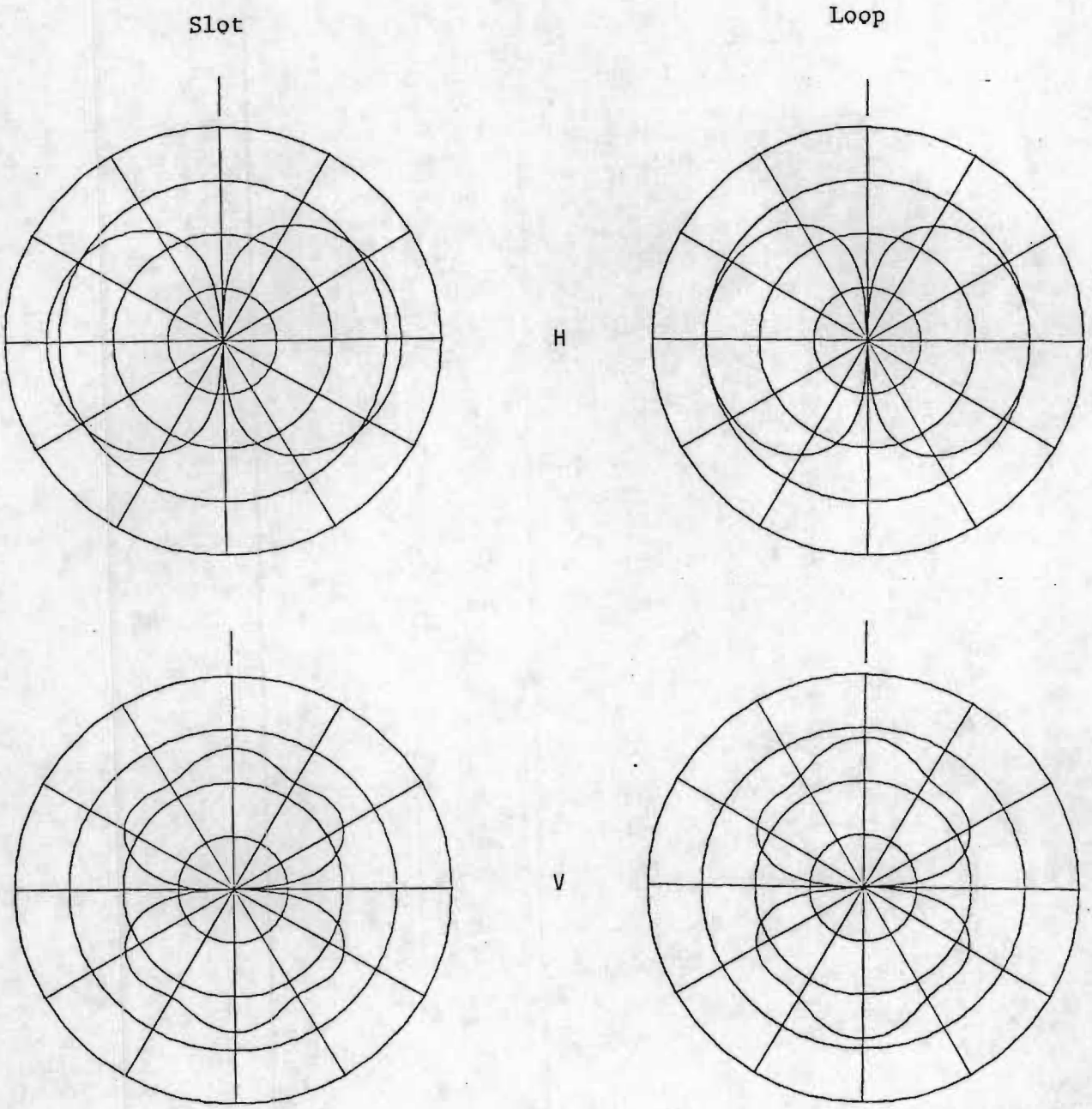

- Ground Plane Patterns
- 10 dB/div
- Hor & Vert. Pol.

Figure 8. Loop - Slot Comparison

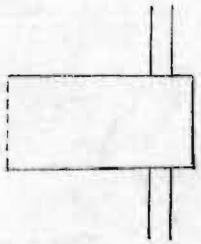

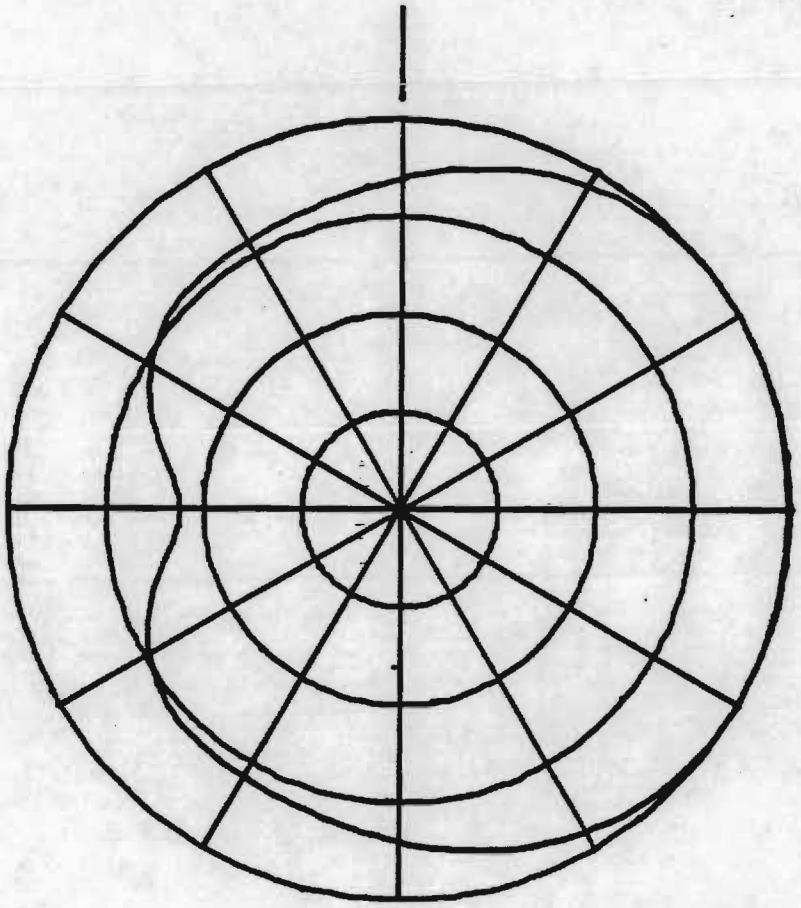

Figure 9. Modified edge slotted waveguide pattern.

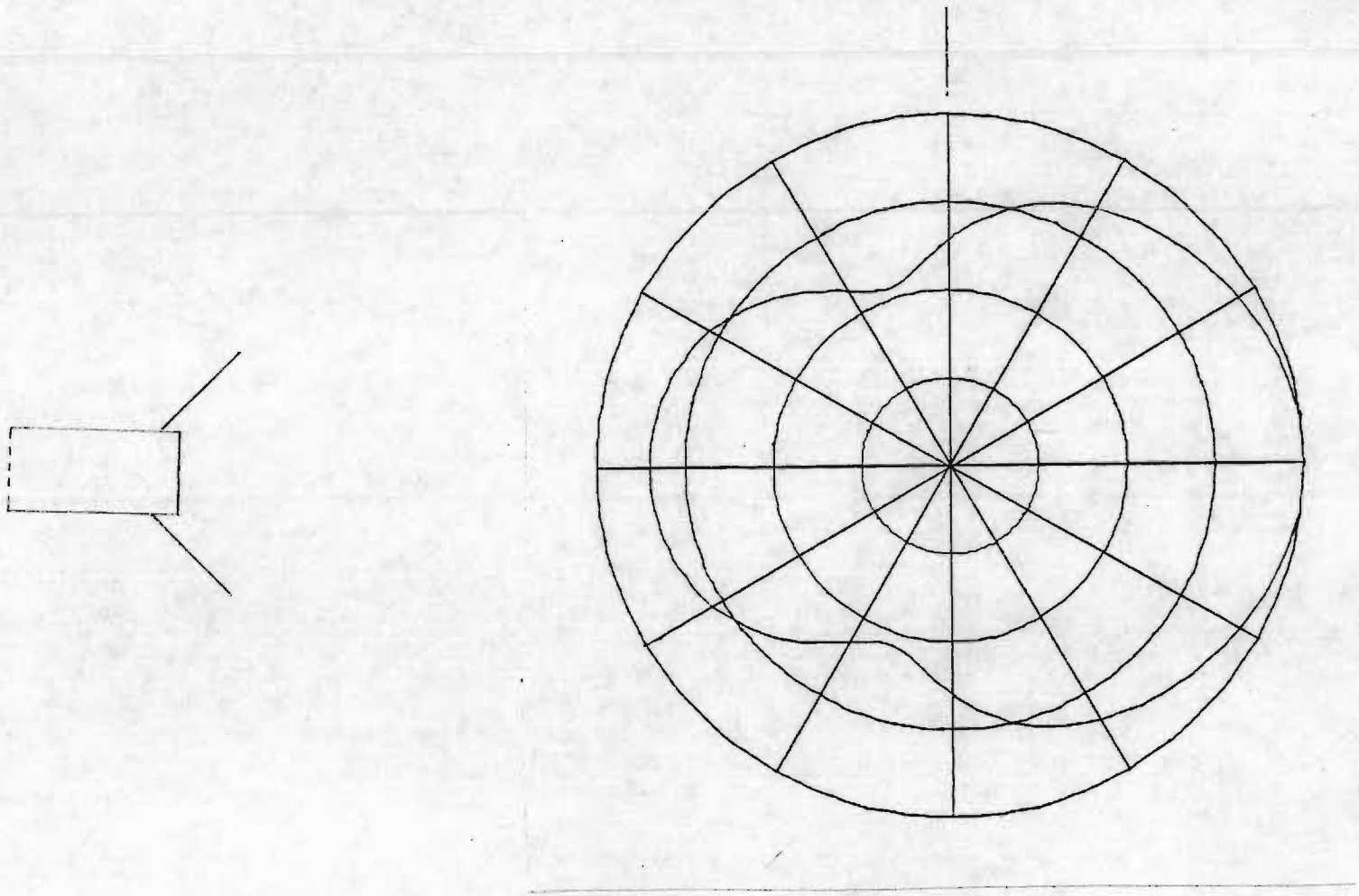

Figure 10. Modified edge slotted waveguide pattern.

slotted waveguide line sources to improve directivity; this type of horn is less desirable than one that requires only vertical or horizontal cuts in the nomex core of the wing. Adding directors results in an additional reduction in back radiation as shown in Figure 11, but the pattern is still far from useful. The directors were 0.45 wavelengths long and were spaced 0.2 wavelengths apart. The pattern when only the four directors were present is shown in Figure 12. Qualitatively, the effects of adding different numbers of directors were the same for the edge slotted waveguide as for the broadwall slotted waveguide.

These results do not necessarily imply that a horizontally polarized rotary wing antenna based on an edge slotted waveguide can not be obtained. In fact, some configurations suggested by later experiments with broadwall slotted waveguide have not yet been tried with edge slots.

2.4 BROADWALL SLOTTED WAVEGUIDE ANTENNA

Several configurations of broadwall slotted waveguide antennas yielded patterns that should be quite useful, depending on final specifications for required elevation coverage. Figure 13 shows a very useful elevation pattern; greater than 20 dB of forward-aft discrimination is obtained for at least 45^{o} of elevation coverage, assuming $\pm 10^{o}$ of wing tilt variation as shown in Figure 14. The antenna configuration can be used to illustrate how an antenna can be integrated with the helicopter wing as shown in Figure 15. The large upper horizontal plate is positioned to be approximately coincident with the skin of the wing, so that it can be in direct contact with, or perhaps represent, the wire grid used to conduct lightning to the rotor hub. A lower lighting conductor is also required, but it does not have to be a grid; parallel longitudinal wires can be used instead. These wires will be essentially invisible to the orthogonally polarized antenna radiation. In the simulation, the directors were 0.45 wavelength wire segments. In the actual antenna, these may be printed on thin dielectric sheets or perhaps they may be formed by cladding on dielectric filaments.

Trough type horns similar to those tried with edge slotted waveguide (Figure 10) increased directivity somewhat, but provided no improvement in discrimination performance over the basic waveguide pattern (Figure 5). The use of a small box horn showed some promise as indicated in Figure 16.

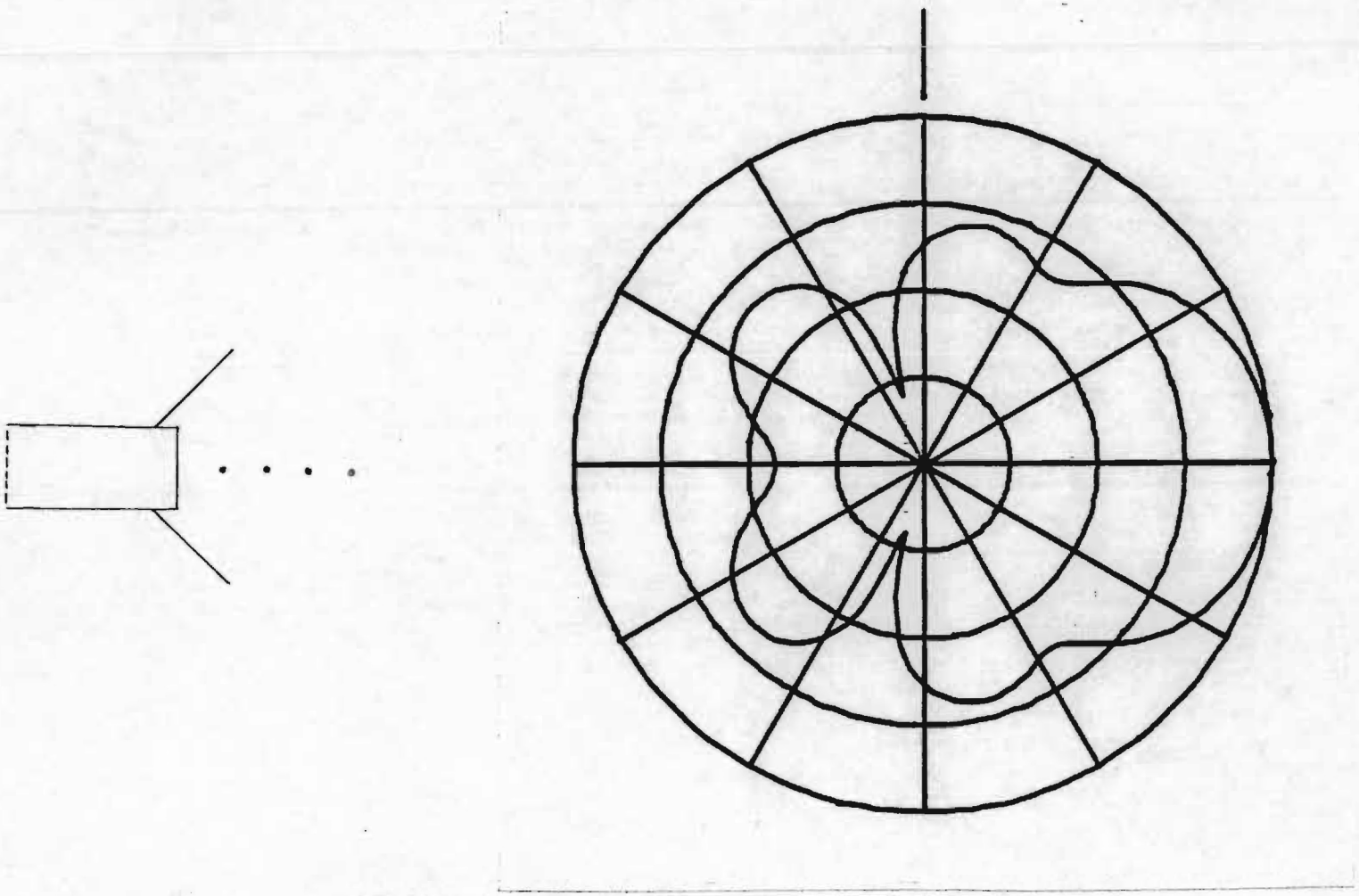

Figure 11. Modified edge slotted waveguide pattern.

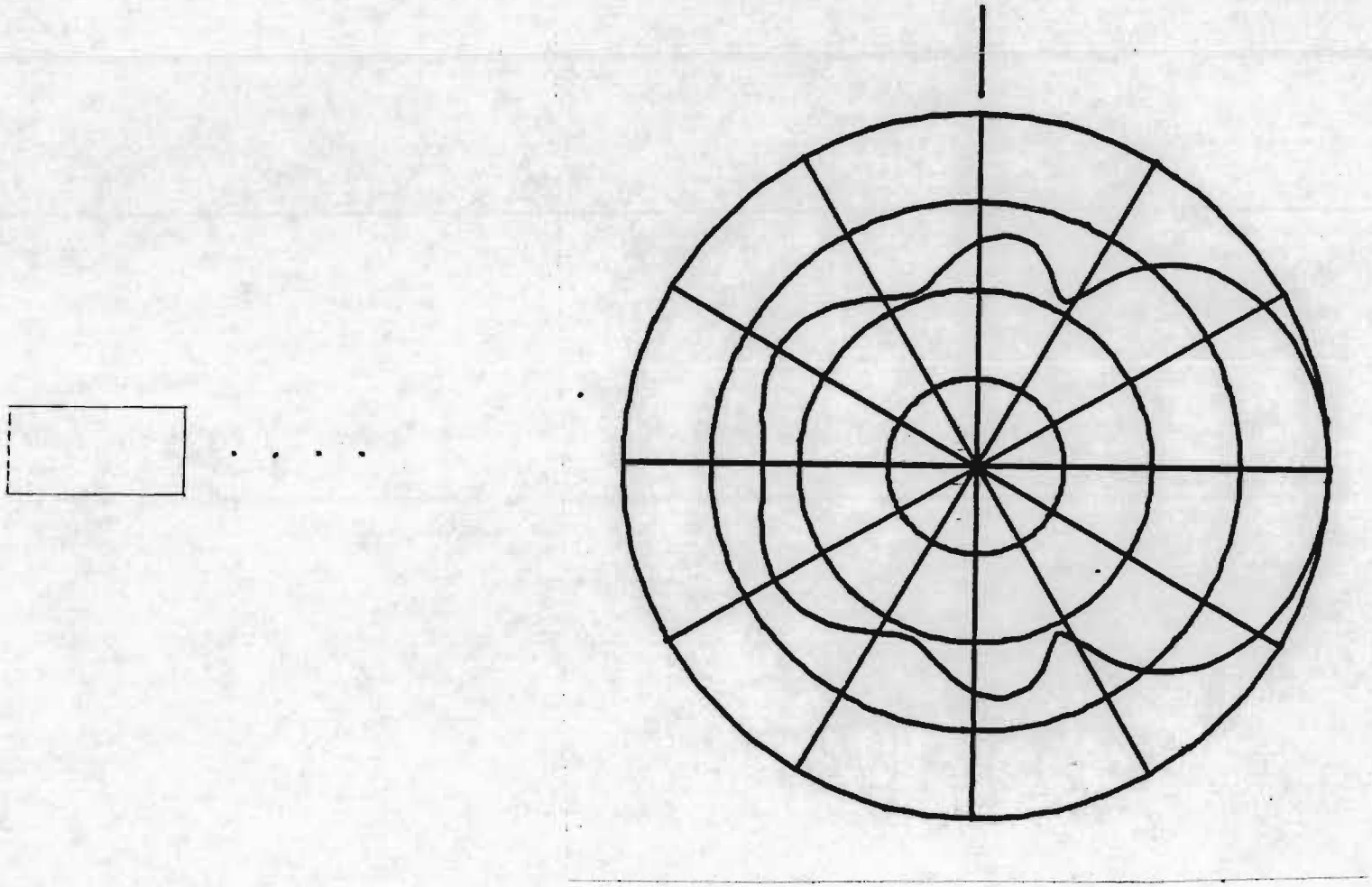

Figure 12. Modified edge slotted waveguide pattern.

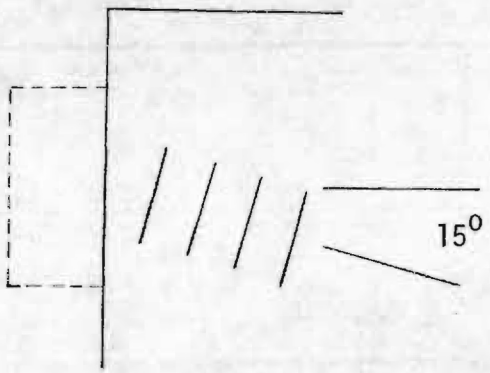

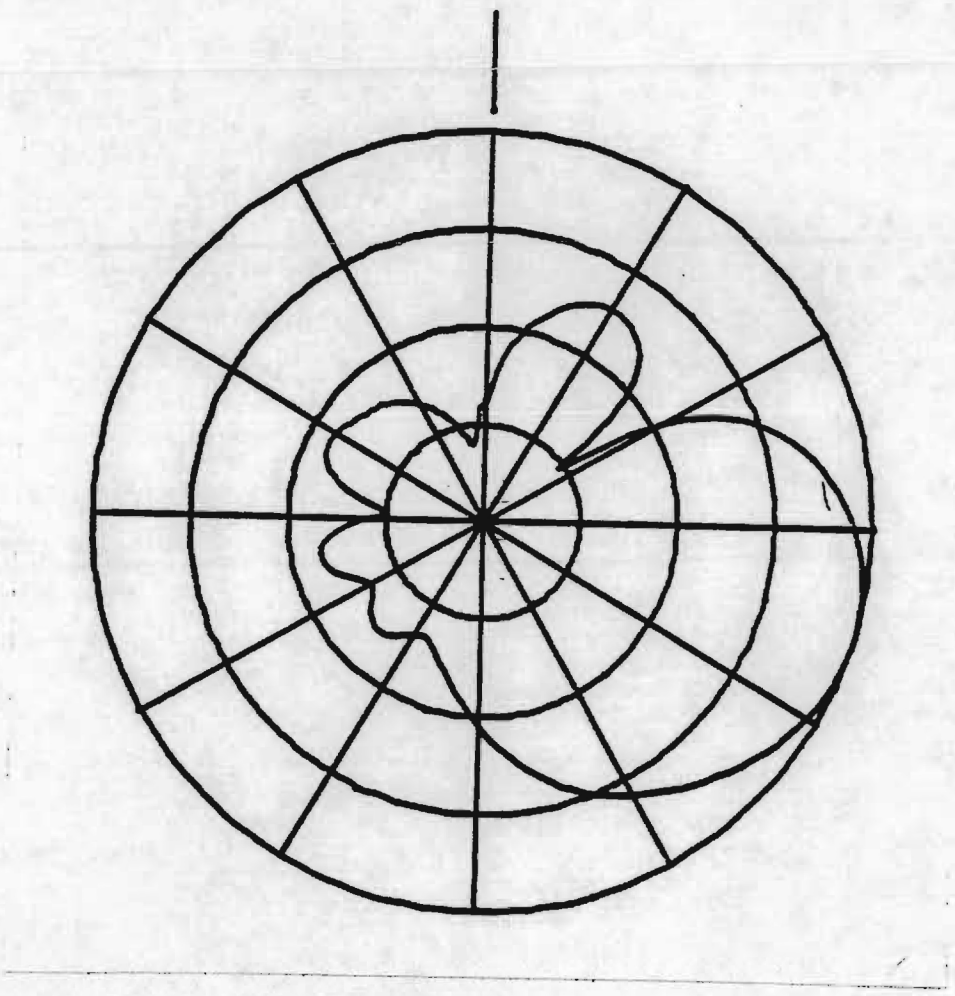

Figure 13. Modified broadwall slotted guide pattern.

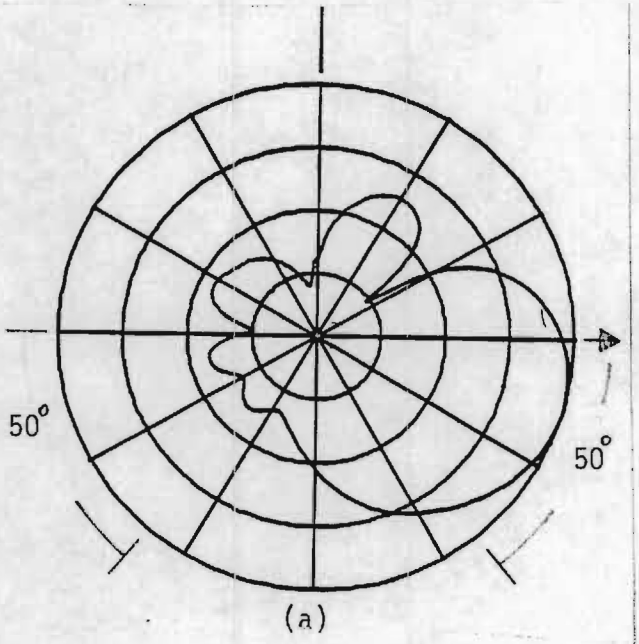

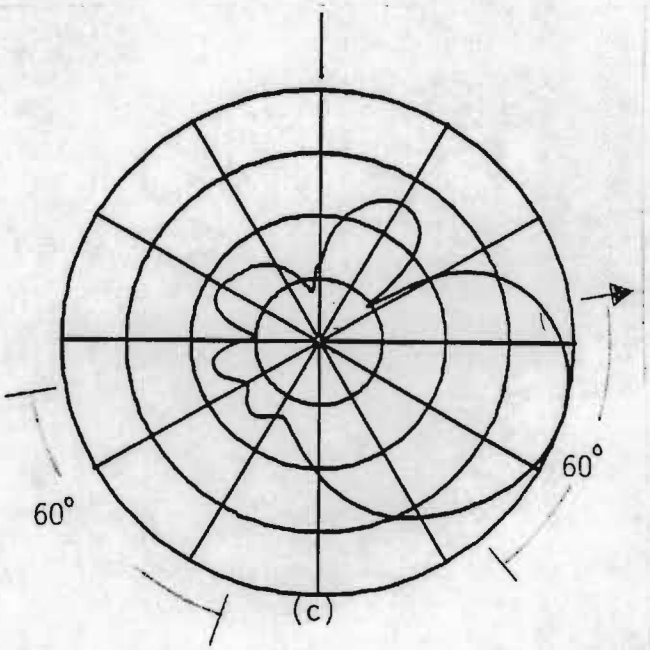

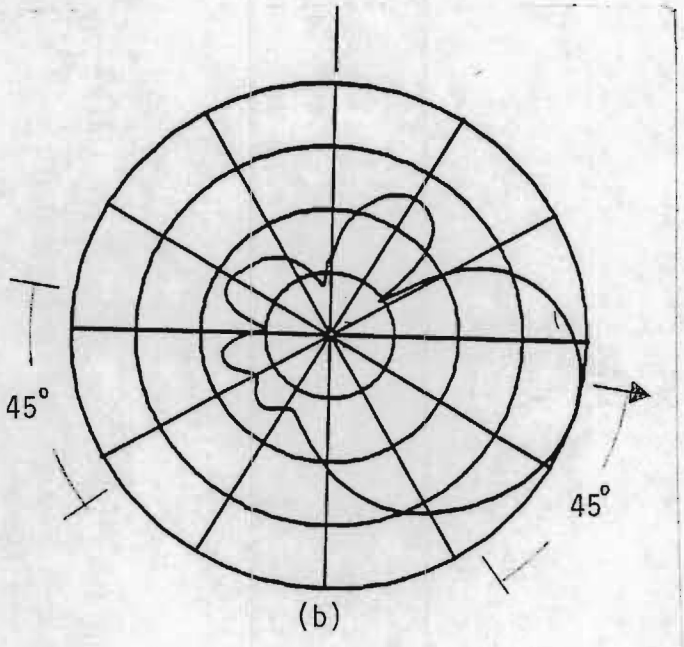

Wing tilt

(a) 0^{o}

(b) $+10^{o}$

(c) -10^{o}

Horizontal

Figure 14. Effect of wing tilt on coverage.

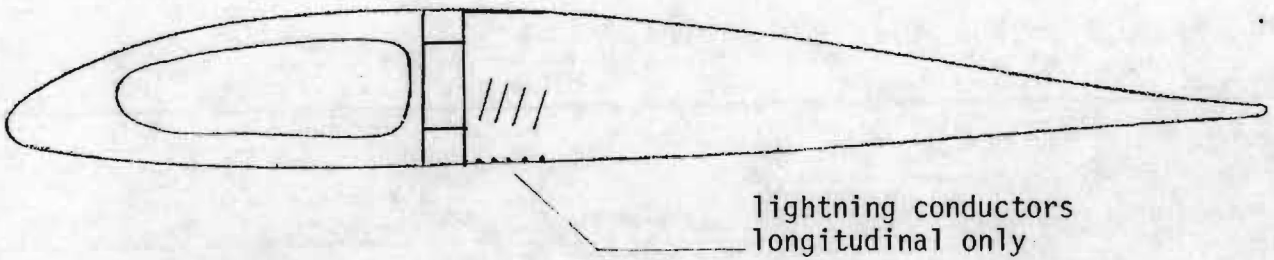

Figure 15. Antenna in wing.

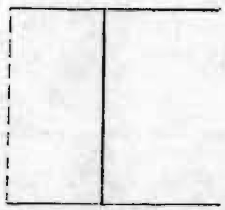

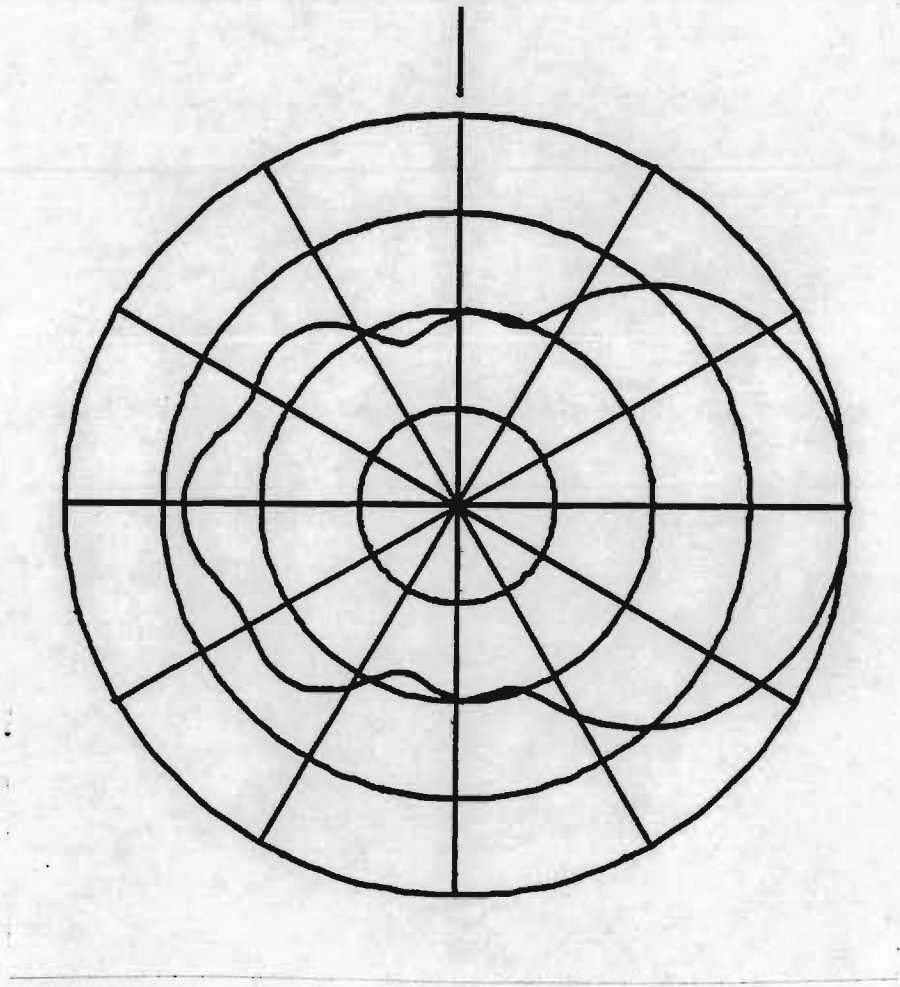

Figure 16. Modified broadwall slotted waveguide pattern.

Figures 17 through 21 show the results of adding one through five directors. The directors were 0.45 wavelengths long and were spaced at 0.2 wavelength intervals. The large back lobe at -180° is typical of an odd number of directors. The use of more than four directors results in an elevation pattern that is too narrow (Figure 21). Figure 22 indicates that the directors alone are not adequate to provide the desired elevation pattern performance.

Figure 20 indicates that the use of four directors can provide a front-to-back ratio of at least 20 dB over 30° to 40° of elevation, allowing for ±10° pitch variation. The elevation interval providing good discrimination performance is limited by the rapid drop in gain below -30° and the large back lobe at -120°. If the antenna could be tilted downward by 30°, good discrimination performance could be obtained over a 70° elevation interval; however, the performance would fall off rapidly with wing pitch variation. Also, tilting the antenna may complicate antenna-wing integration.

Figure 23 illustrates the pattern when wire grid lightning conductors are above and below the antenna. The large horizontal plates are approximately coincident with the skin of the wing. The front-to-back ratio of this antenna is very good (up to 55° of elevation interval) when the wing is horizontal or tilted downward, but drops off as the wing is tilted upward. About 30° of elevation coverage is achieved for a +10° wing tilt.

Figure 24 illustrates the pattern obtained when the front plate of the waveguide is extended upward to meet the horizontal plates representing the lightning conductor grids. Performance is improved somewhat over that indicated in Figure 20 because of the reduction in the back lobe at -120°. The elevation interval for more than 20 dB foward-to-aft discrimination varies from 35° for a +10° wing tilt to 45° for a -45° wing tilt. As with the configuration of Figure 20, the elevation interval for good discrimination can be extended to 70° by tilting the antenna downward by 30°. Figure 25 shows the pattern that would be obtained if the directors were removed.

The lower plate was removed in an attempt to increase the gain in the lower forward quadrant, but this only increased the back lobe level as shown in Figure 26. The lower plate is effectively removed by replacing the lower lightning conductor grid with parallel longitudinal wires. Increased gain in the lower forward sector was obtained by tilting the directors downward by 15°

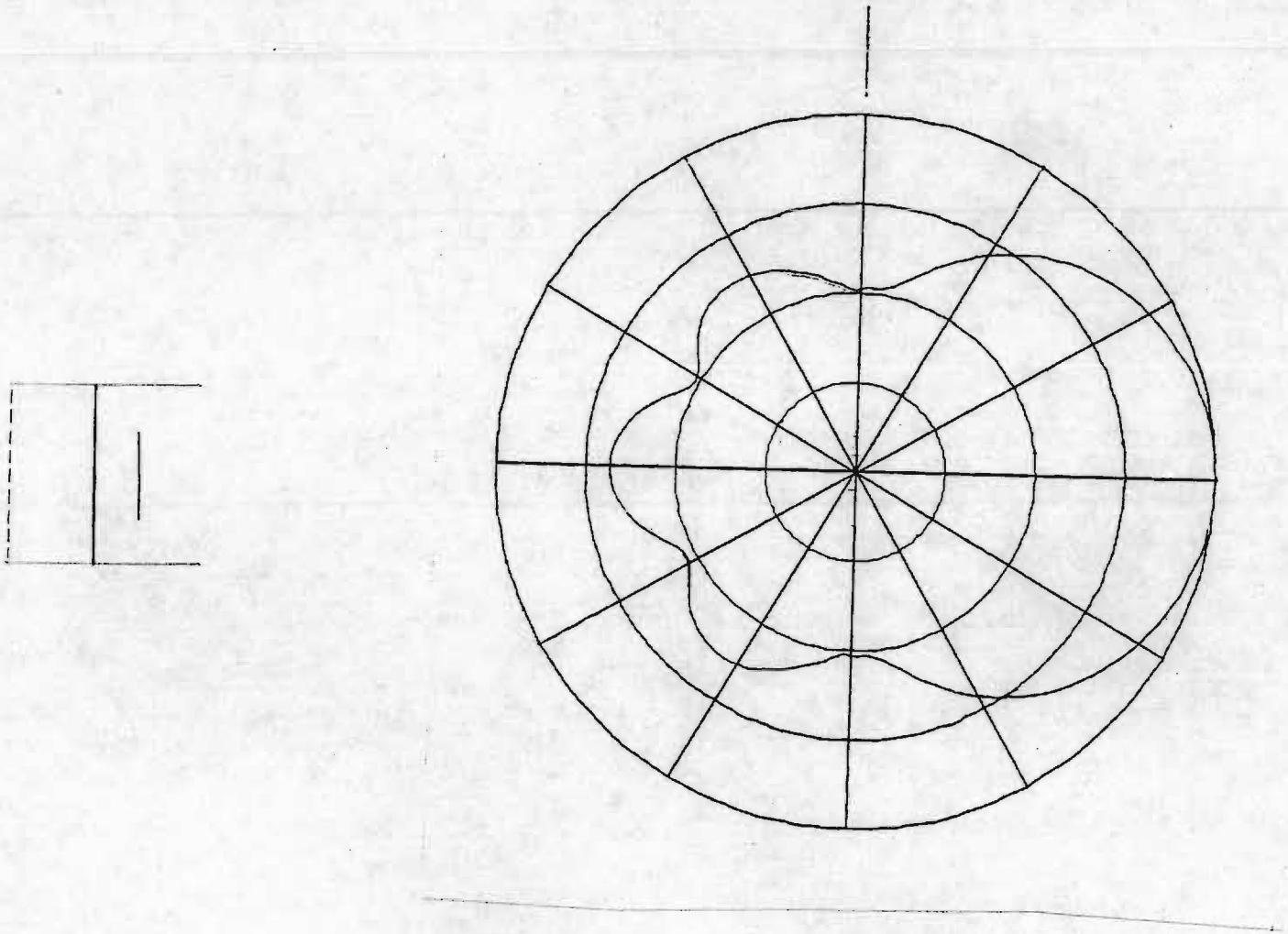

Figure 17. Modified broadwall slotted waveguide pattern.

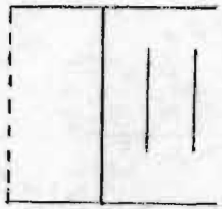

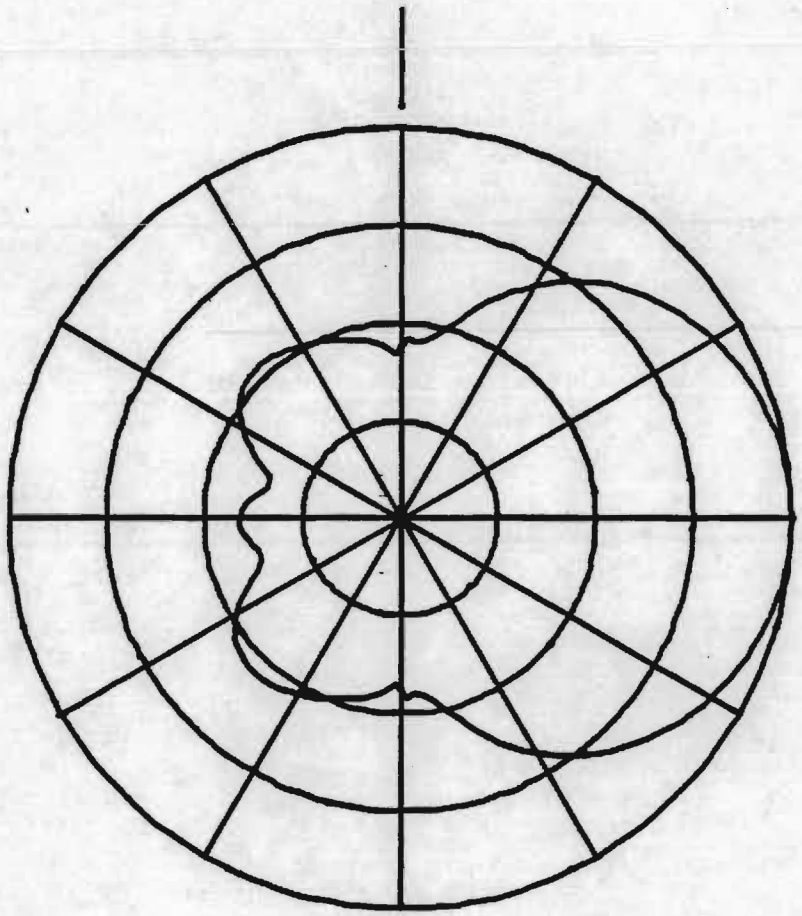

Figure 18. Modified broadwall slotted guide pattern.

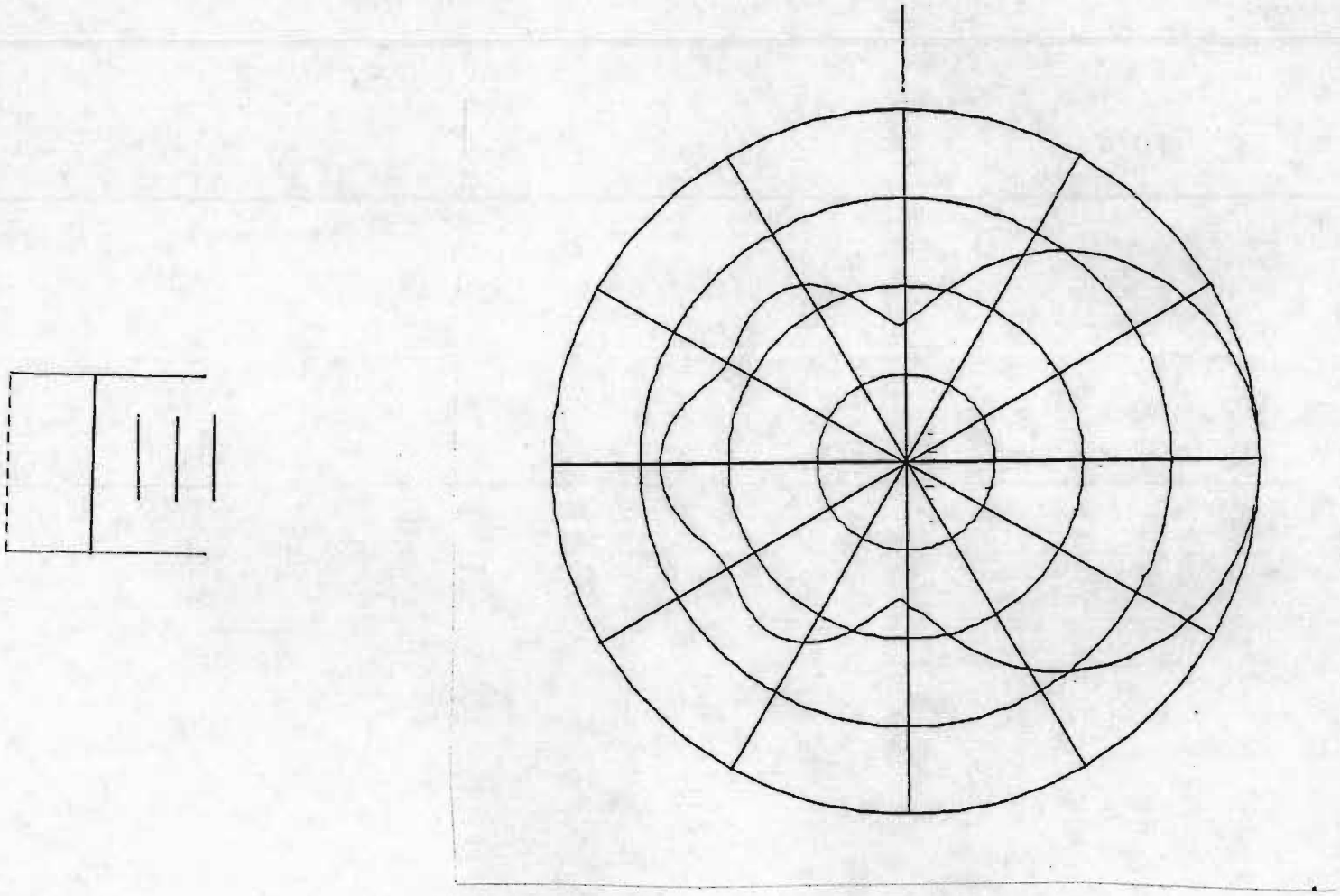

Figure 19. Modified broadwall slotted guide pattern.

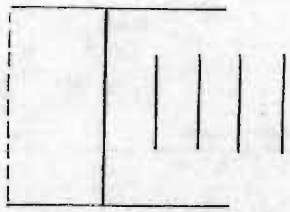

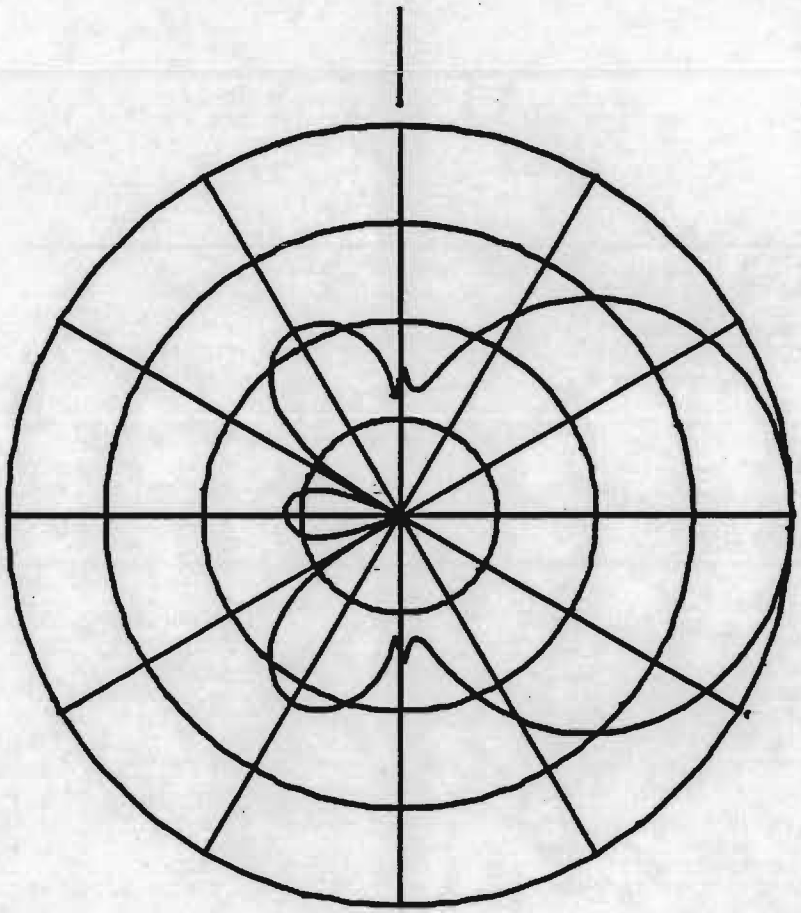

Figure 20. Modified broadwall slotted guide pattern.

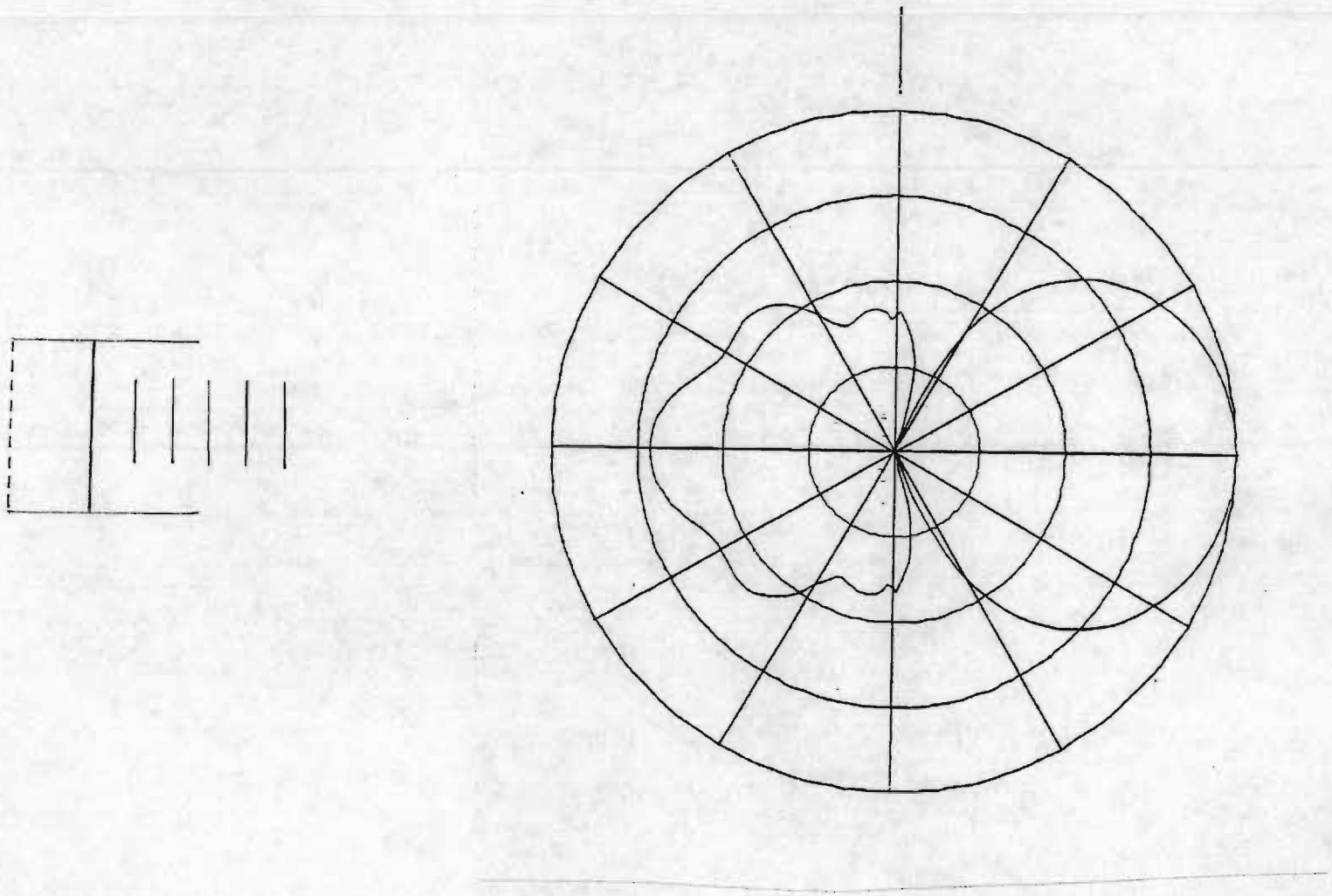

Figure 21. Modified broadwall slotted guide pattern.

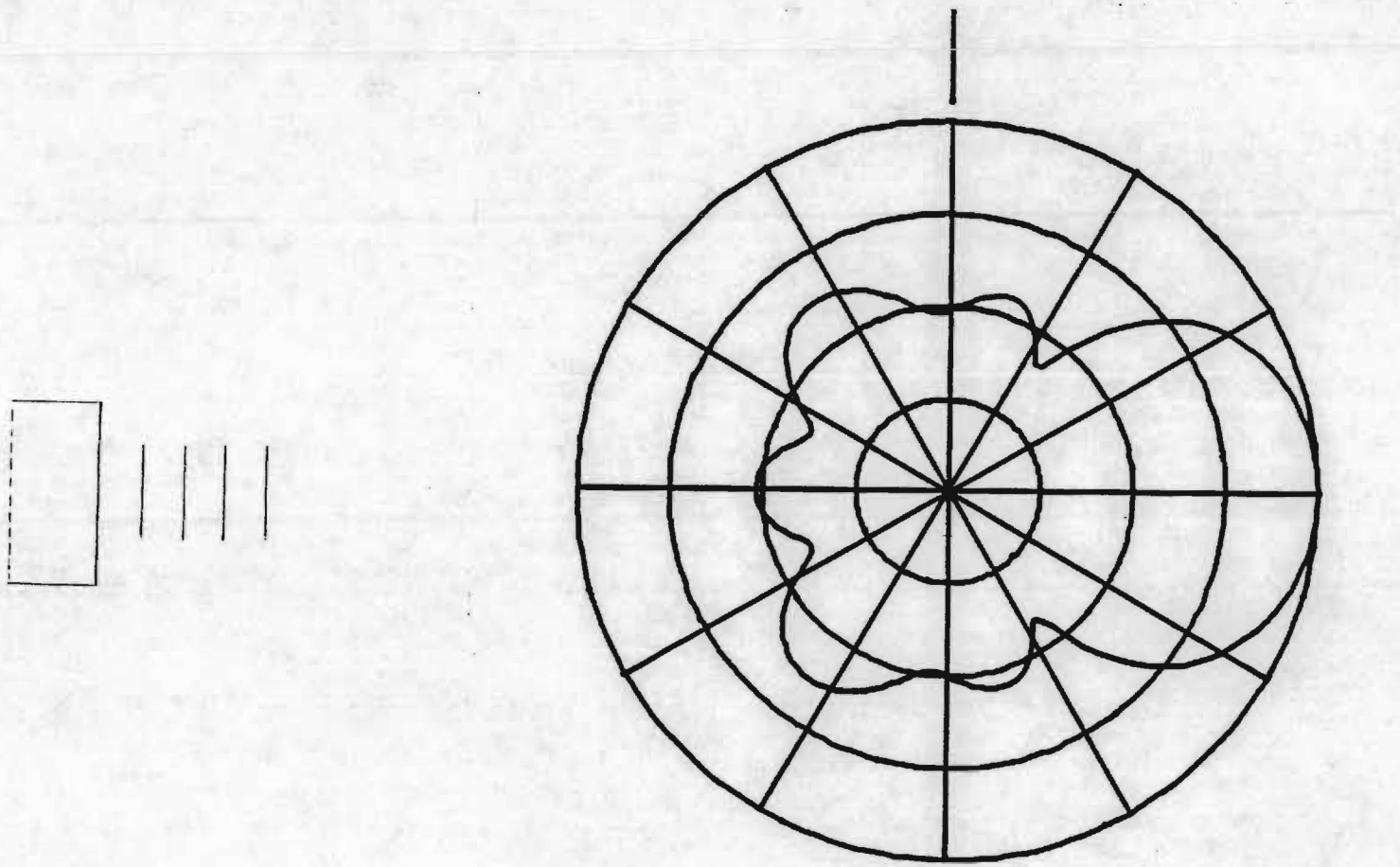

Figure 22. Modified broadwall slotted guide pattern.

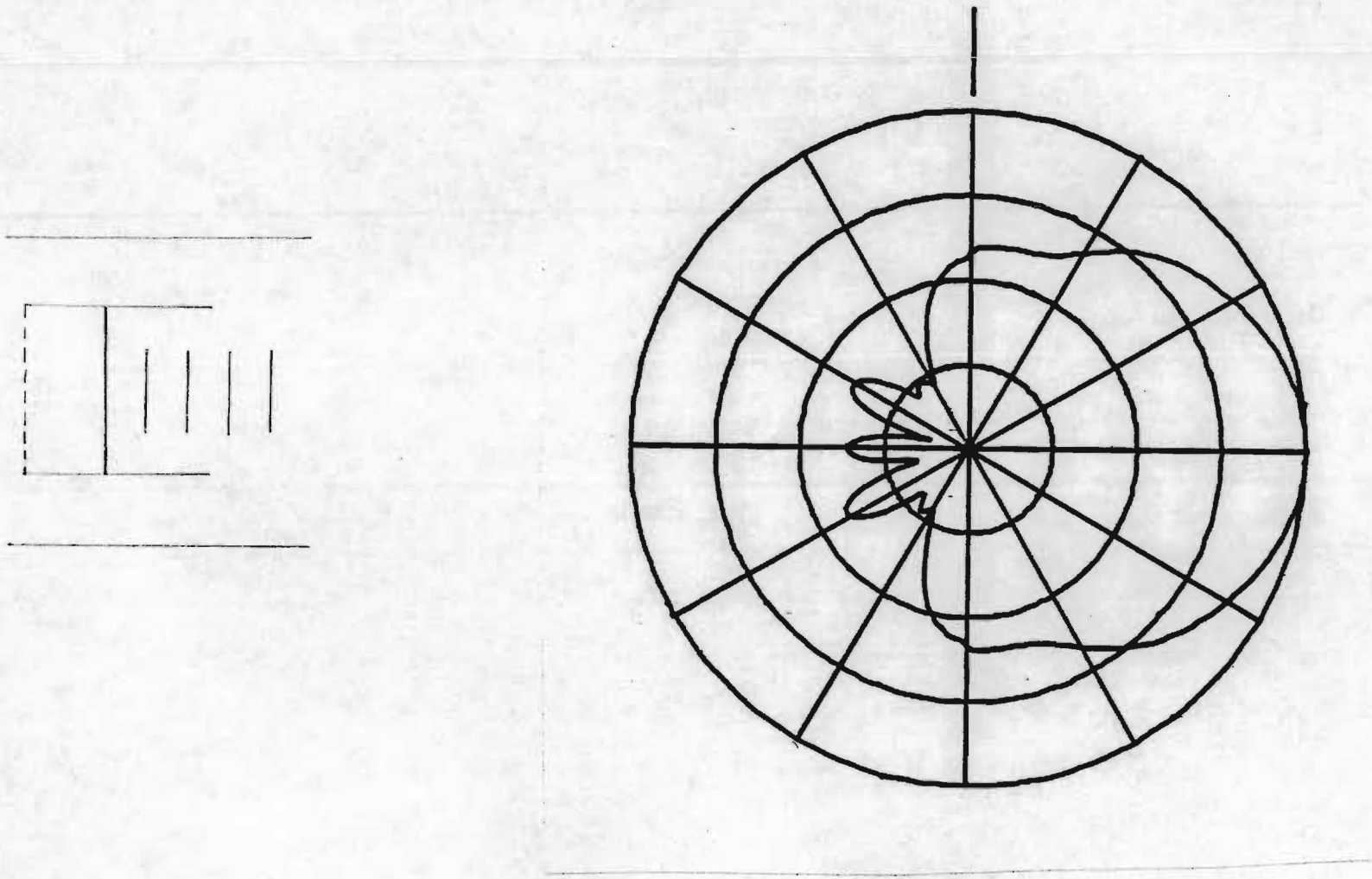

Figure 23. Modified broadwall slotted guide pattern.

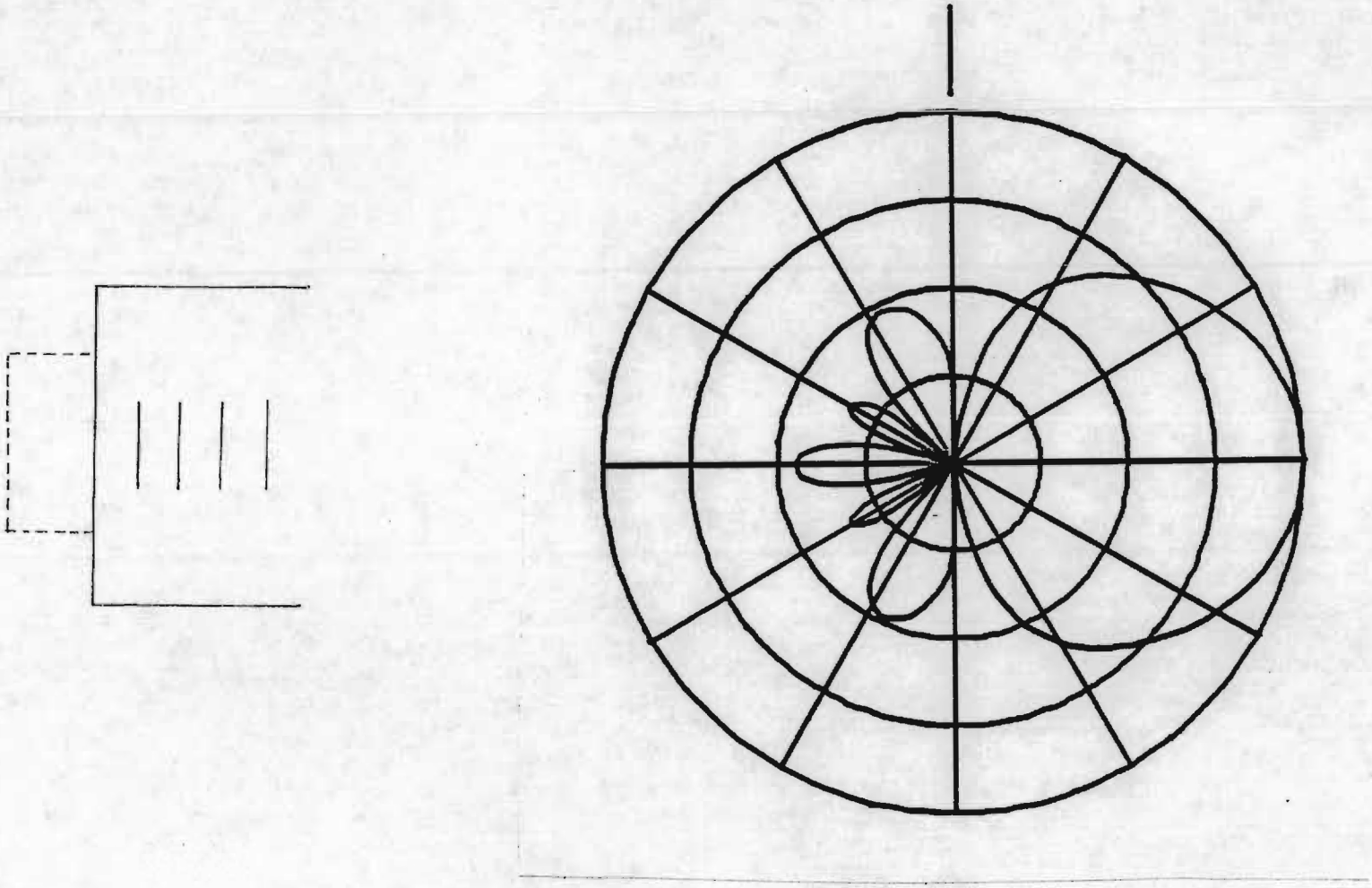

Figure 24. Modified broadwall slotted guide pattern.

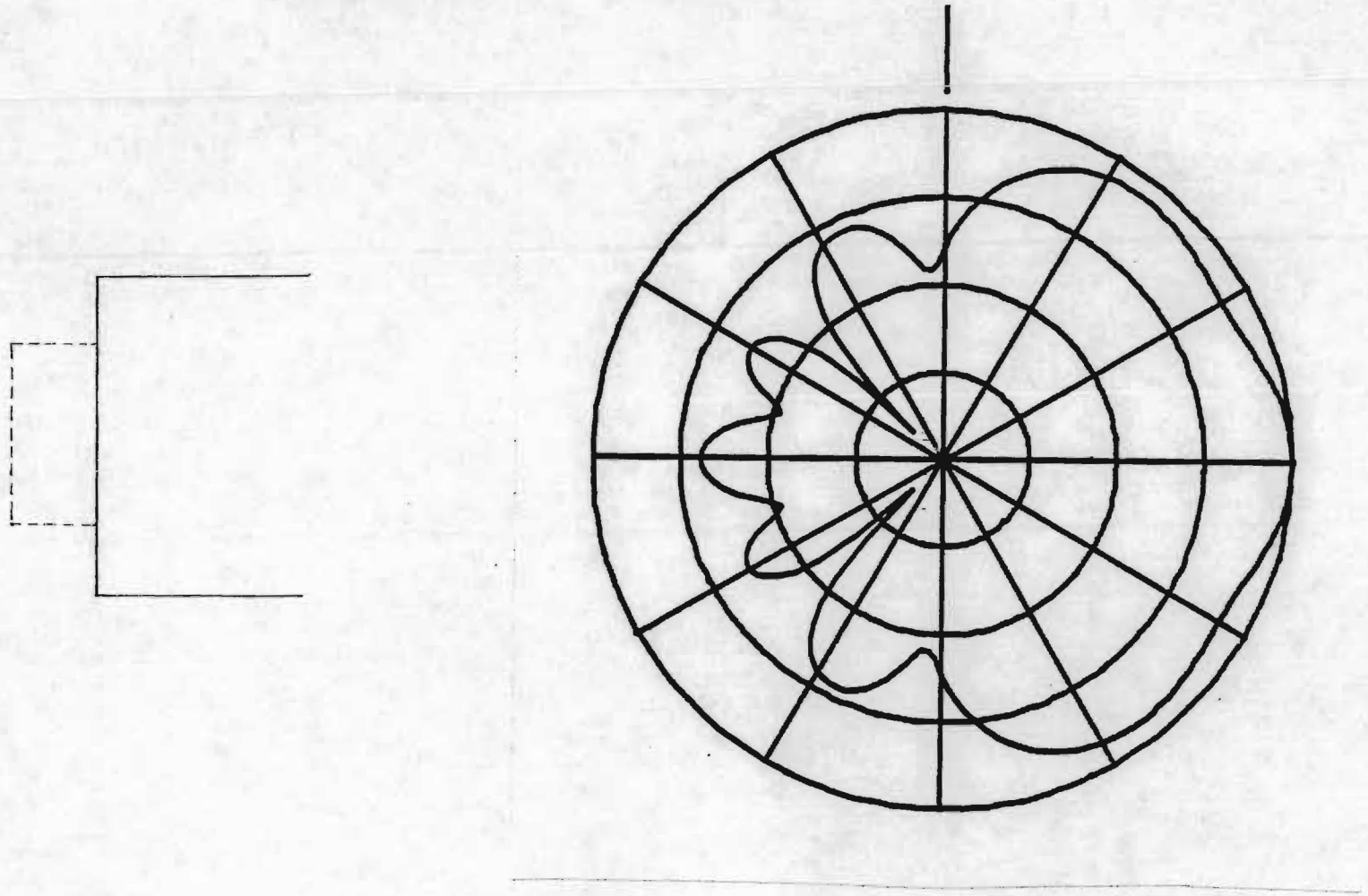

Figure 25. Modified broadwall slotted guide pattern.

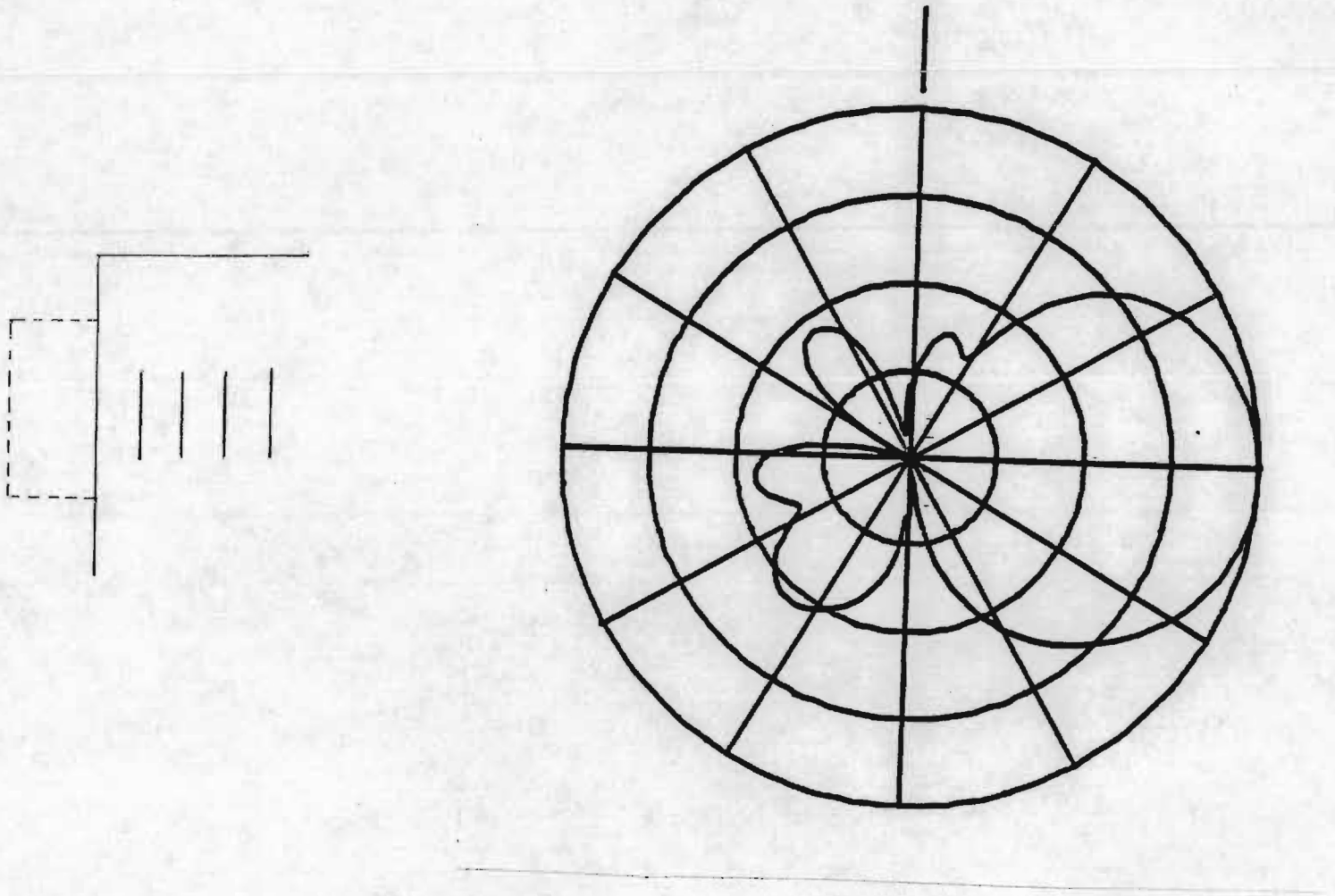

Figure 26. Modified broadwall slotted guide pattern.

as shown in Figure 13. Tilting the directors downward 30° resulted in too large a gain loss at 0° as shown in Figure 27.

Although many more antenna configurations and variations could have been examined, this limited analytical study demonstrates that a helicopter rotary wing antenna is a practical consideration. The next logical step is an empirical development effort.

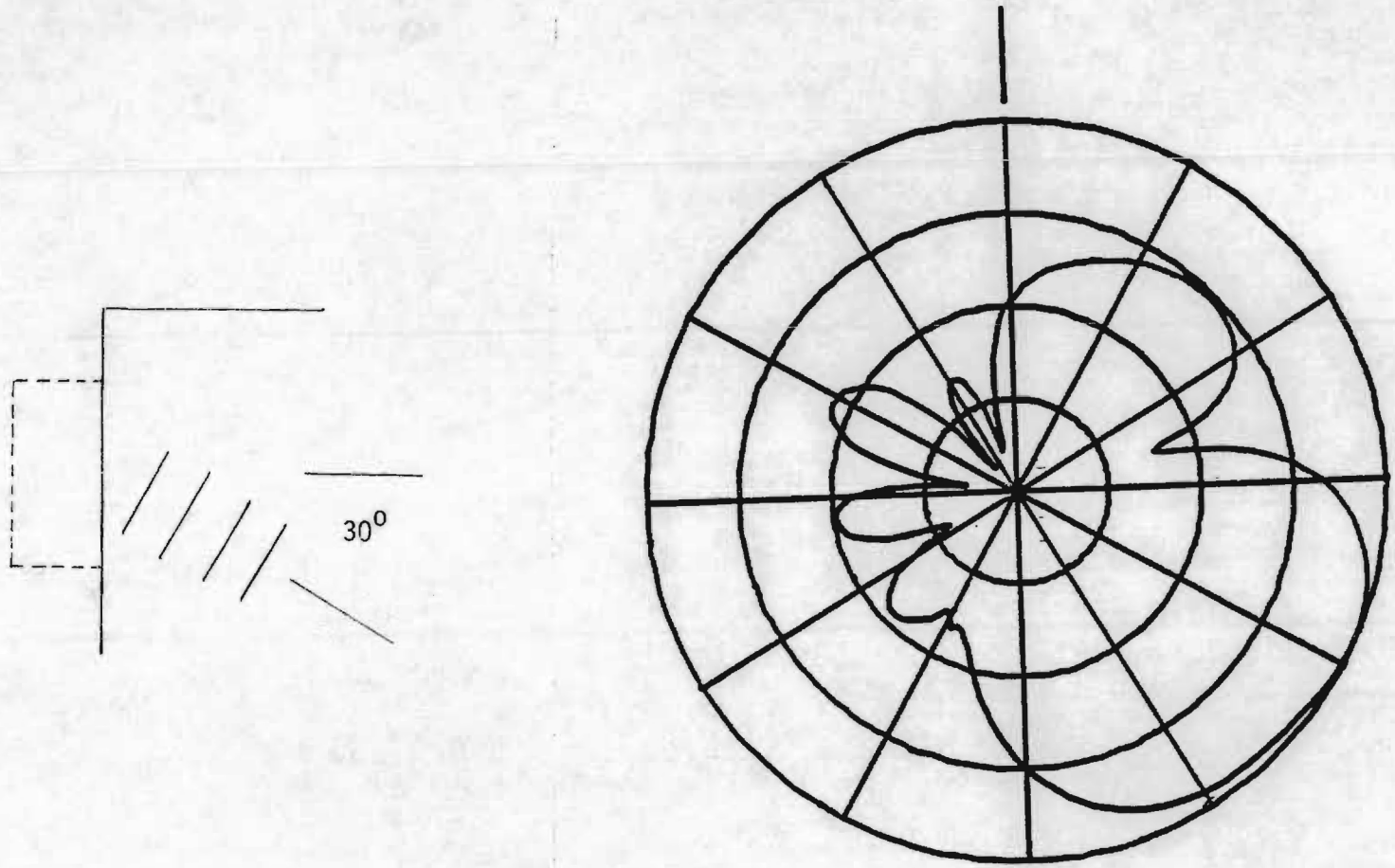

Figure 27. Modified broadwall slotted guide pattern.

SECTION 3

DUAL FREQUENCY FORWARD LOOKING RADAR ANALYSIS

3.1 MILLIMETER WAVE RADAR PERFORMANCE CONSIDERATIONS

3.1.1 ANGULAR RESOLUTION

Millimeter wave frequencies for radar offer improved angular resolution and reduced antenna size in relation to lower frequency radars. A 12-inch, 95 GHz antenna provides the same beamwidth as a 10-foot antenna at 9.5 GHz. Since beamwidth is linearly related (inversely proportional) to antenna size and frequency, a 10:1 increase in frequency provides a 10:1 reduction in beamwidth or, alternately, a 10:1 reduction in antenna size.

A helicopter, 10-foot, X-band rotor blade antenna will provide an azimuth beamwidth of approximately 0.5 degrees, but the elevation beamwidth will be at least 45 degrees. Since a helicopter can not accommodate a 10-foot tall rotor blade antenna, commensurate elevation resolution must be provided some other way.

Consider an off-shore drilling platform with a helipad nestled among buildings, towers, and other structures. Below the platform are posts, pilings, and other structures. At every range there will be radar scatterers at many angles. Any technique that merely computes the centroid of these scatterers will be of little benefit in inspecting the landing area. In this case, image quality radar data are needed.

Where the earth surface and points of interest can be assumed flat, elevation angle is simply a function of platform altitude and range. Thus, the conventional range-by-azimuth radar plan position indicator (PPI) map display ignores elevation angle.

Elevation monopulse processing is a technique that can measure elevation angle under some conditions. With monopulse processing, the angle to the centroid of each range cell is computed. As long as there is only one radar scatterer per range bin, this technique will provide a useful measure of angle. However, there is no substitute for a narrow beamwidth. Consider: if monopulse processing were capable of always resolving elevation, would it not be capable of resolving azimuth? Since for image quality data elevation resolution is as important as azimuth resolution, the radar antenna needs to be a planar aperture, not just a line source.

Image quality data can be approached with a high resolution millimeter wave radar. An 18-inch diameter, forward looking 95 GHz radar with 0.5^{o} x 0.5^{o} beamwidth and a 20 nanosecond pulse will provide a resolution better than 10-feet (azimuth, elevation, and range) when the range is less than 1,115 feet. With this resolution, a autonomous helicopter landing should be possible.

3.1.2 WEATHER LOSSES

The advantage of millimeter wave (MMW) radar is better angle resolution or smaller antennas. The disadvantage of MMW radar is its susceptibility to degradation by weather. MMW radar falls between optical and X-band systems in its ability to penetrate weather.

The radar equations used to support the following analyses are given in Table 1; the terms are defined in Table 2.

MMW radar is finding many applications in moderate weather (4 mm/hr rain, 100 m fog) where its penetration is much superior to optical and infrared systems, but 25 mm/hr rain is severe, especially at the higher MMW frequencies.

Figure 28 plots rain attenuation (dB/km) and volumetric backscatter coefficient (m^2/m^3) as a function of rain rate at 95 GHz. As shown in the plot, a 95-GHz radar will suffer about 8 dB/km (round trip) atmospheric loss in a moderate rain (4 mm/hr), but the loss will be more than 25 dB/km in a heavy rain (25 mm/hr).

The impact of 25 dB/km signal loss due to heavy rain may be appreciated by comparing system performance with and without the rain. A 95-GHz radar designed for a detection range of 1 km in 25 mm/hr rain will have a clear air range of 4 km. A 95-GHz radar designed for a detection range of 2 km in 25 mm/hr rain would have a clear air range of 21 km. A 95-GHz radar capable of detecting a target at 4 km in heavy rain would detect the same target at a range of 100 km when there is no rain.

Figure 28 plots the visibility of a reference 1-square meter (1 m^2) target in 25 mm/hr rain using a MMW radar operating at 95 GHz with an 18-inch antenna and a 20 ns pulse width. With a 50 MHz IF bandwidth, the radar is capable of approximately a 3 meter range resolution. A 7 dB receiver noise figure and 6 dB of system losses are assumed. The radar performance for both

TABLE 1. RADAR EQUATIONS

OUTPUT SIGNAL-TO-NOISE RATIO

(1.1) $$S/N = \frac{P\,G^2\,\lambda^2}{(4\pi)^3 kTBN_f L_s L_w R^4}$$

RADAR CROSS SECTION OF HOMOGENEOUS TERRAIN

(1.2) $$\sigma_G\,(m^2) = \sigma^o\,\frac{c\tau}{2}\,R\sin\theta \quad (\sigma^o = \text{Reflectivity})$$

RADAR CROSS SECTION OF RAIN

(1.3) $$\sigma_r\,(m^2) = \eta\,\frac{c\tau}{2}\,(R\sin\theta)^2$$

(η = volumetric reflectivity)

WEATHER LOSS[3]

(1.4) $$L_w\,(dB) \simeq 2R\,[0.22 + 1.66\,(rr)^{0.64}] \quad @\ 95\ GHz$$

WEATHER REFLECTIVITY[4]

(1.5) $$\eta\,(m^2/m^3) \simeq 1.5 \times 10^{-5}\,(rr)^{1.103}$$

TABLE 2. RADAR TERMS

P	= Peak Transmitted Power (W)
B	= Received Bandwidth (Hz)
G	= Antenna Gain
λ	= Wavelength (m)
σ	= Radar Cross Section (m^2)
kT	= Noise Temperature (-204 dBw/Hz)
N_f	= Receiver Noise Figure
L_s	= System Losses
L_w	= Atmospheric Loss
R	= Range (km)
θ	= Antenna Beamwidth (pencil beam)
rr	= Rain Rate (mm/hr)
τ	= Pulse Length (s)
C	= Propagation Velocity 3×10^9 m/s

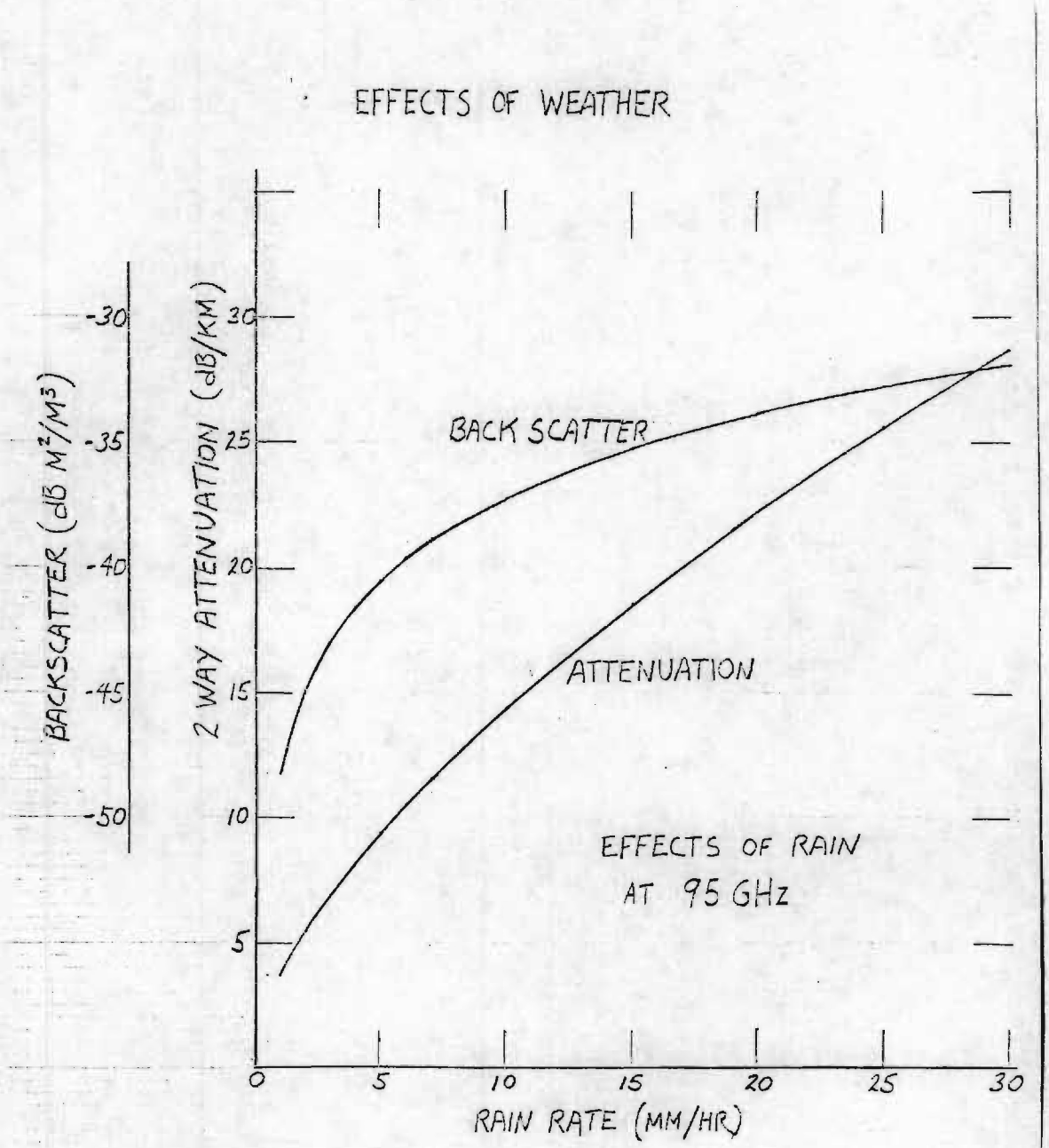

Figure 28. Effects of weather.

a 1 kW (peak) transmitter and a 10 W transmitter are plotted for comparison. At a range of 1 km, the 1-kW transmitter provides a +25 dB signal-to-noise (S/N) ratio; the 10-W transmitter provides a 5 dB S/N ratio. At a range of 2 km, the 1-kW radar provides a 0 dB S/N ratio; the 10-W radar provides a 0 dB S/N at a range of about 1.2 km. At 25 dB/km attenuation, each additional kilometer of radar range necessitates a 300:1 increase in transmitter power.

3.1.3 WEATHER CLUTTER

In addition to absorbing the radar energy, rain also reflects it. Rain backscatter can obscure radar targets of interest. The amplitude of the radar signal returned by rain is proportional to the antenna beam area, the radar pulse length, and the rain backscatter coefficient. The backscatter curve in Figure 29 shows that the volumetric backscatter from 25 mm/hr rain is almost ten times greater than from 4 mm/hr rain at 95 GHz.

Figure 29 is a plot of the signal-to-rain backscatter ratio for the reference radar example. At 95 GHz, the return from a 1 m^2 meter target will be larger than the return from a volume of 25 mm/hr rain for ranges out to 2 km. The signal-to-rain ratio margin, however, is not very much; the margin is only 3 dB at a range of 2 km and 9 dB at a range of 1 km. The signal-to-rain ratio does not exceed 10 dB until the range is decreased to less than 0.8 km.

3.1.4 SIGNAL MARGIN

Figure 30 illustrates the combined signal-to-interference effects of thermal noise and rain. Here is plotted the signal-to-interference ratio, which is the ratio of the target signal to the sum of receiver noise plus rain return (given a 1 m^2 target in 25 mm/hr rain). Notice the difference between the curves for the 1-kW system and the 10-W system. For a 0.5 km range, there is little difference (less than 1 dB) in the curves; the radar is clutter limited, i.e., the rain backscatter swamps out the effects of receiver noise. For the 1 m^2 target at a range of 1 km, the 1-kW radar has a 10 dB signal margin, 5 or 6 dB better than the 10-W radar signal margin. The signal margin for the 1-kW system remains above 0 dB for ranges out to about 1.9 km, whereas the signal margin for the 10-W system decreases to 0 dB at a range of about 1.2 km. At a range of 2 km, the 1-kW system has a 20 dB signal margin advantage over the 10-W system.

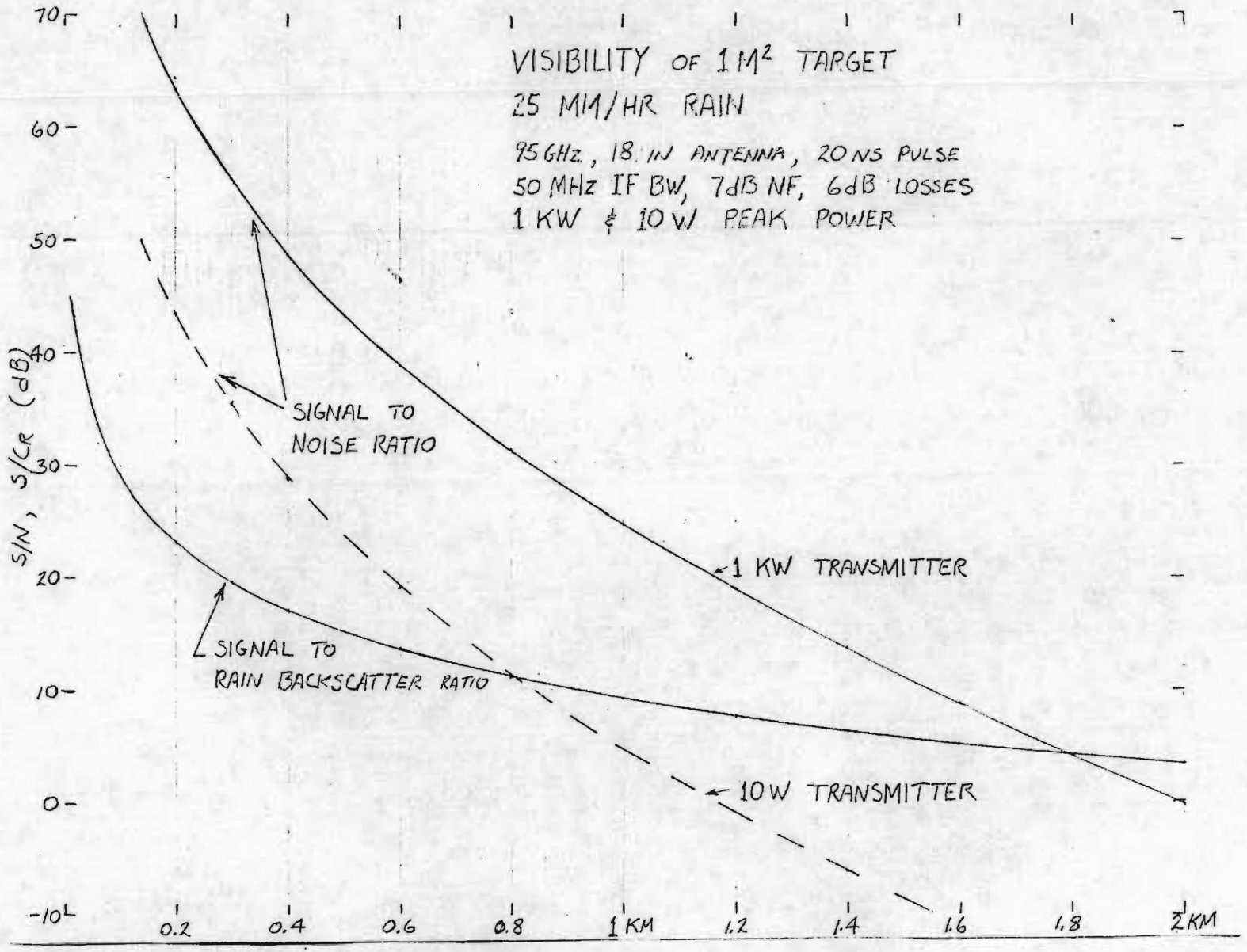

Figure 29. Visibility of 1 M^2 target.

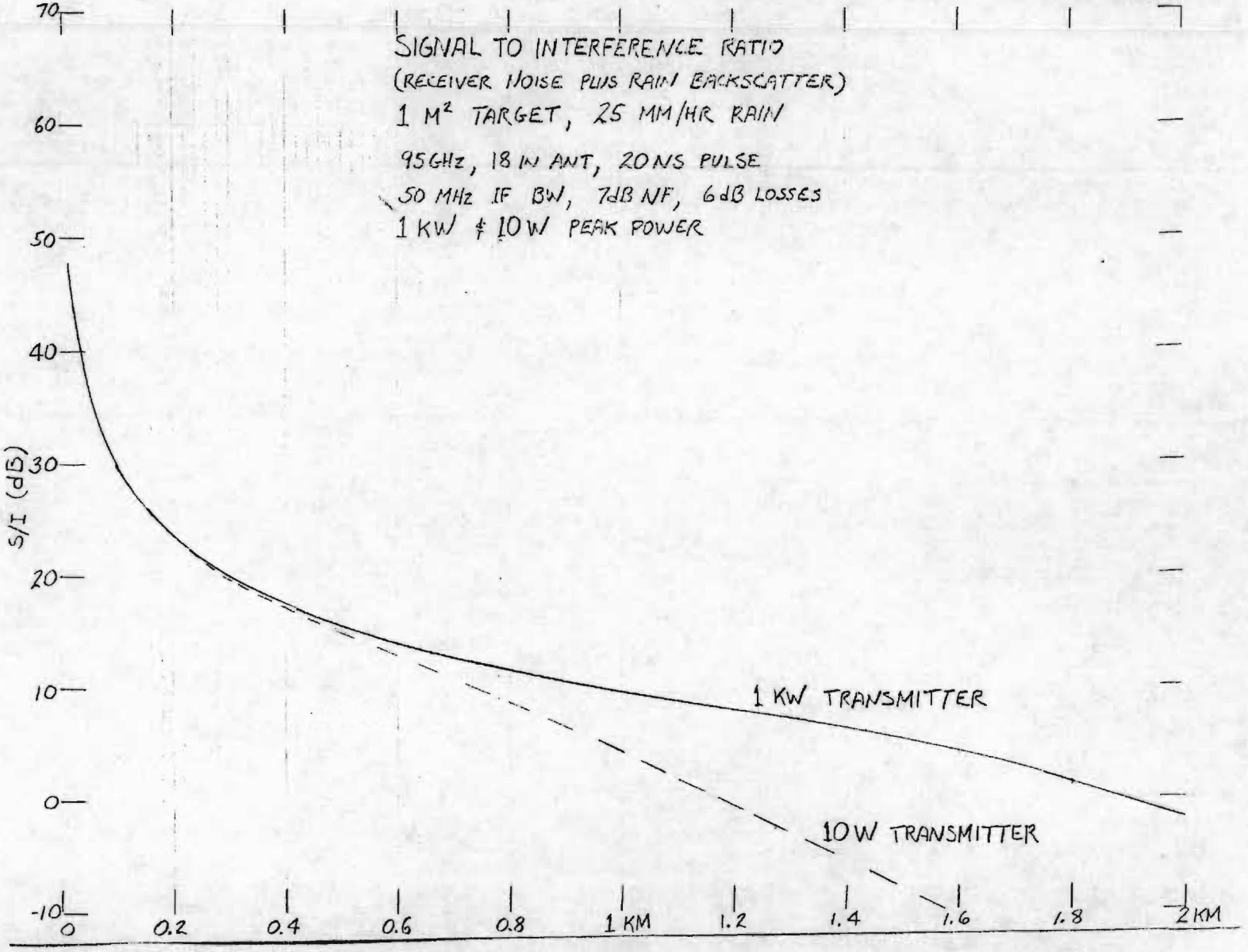

Figure 30. Signal-to-interference ratio.

If the detection criteria are set to correspond to a 10 dB signal-to-interference ratio, the 1 m^2 target can be detected in 25 mm/hr rain at ranges out to about 1 km by the 1-kW radar or 0.75 km by the 10-W radar. With some additional signal processing, the 1-kW radar has the potential for detecting a 1 m^2 target at ranges out to 1.5 km, but the 10-W radar cannot be expected to achieve a detection range of 1 km for the 1 m^2 target. However, a corner reflector, or a side of a building, or part of a drilling platform can be several hundred square meters, in which case a 10-W system would be adequate. Unfortunately, since a smooth, flat landing site will not provide a useful radar return, the existence of the surface cannot be verified by radar.

3.1.5 MAPPING SENSITIVITY

For applications where there may be little radar contrast between the landing sites and the surrounding terrain, finding acceptable sites could be a problem. Look at the problem of trying to land on a runway situated in a marshy field. Since the runway itself will provide little backscatter (the scatter is mostly forward scatter), the runway will appear as a black hole on the radar display. In this case, the radar operator will have to look for the border between the terrain and the smooth runway.

The effective radar cross section of terrain is a product of the area resolved by the radar and the reflectivity of the terrain. The backscatter coefficient (σ^o) of the terrain is a function of its roughness, dielectric constant, and loss tangent. The physical size of the illuminated terrain, as it appears to the radar, is a function of the antenna beamwidth, depression angle, and the range resolution.

Figure 31 is a plot of the effective radar cross section of terrain as a function of reflectivity and distance for the example 95-GHz radar. Typical terrain has a reflectivity between -10 dB and -30 dB. Thus, at a range of 1 km, the terrain should have a cross section of +3 dB square meters, or twice as big as a 1 m^2 target at 1 km. A σ^o of -20 dB, on the other hand, results in a cross section of -6 dBsm (i.e., 0.25 m^2), and a σ^o of -30 dB results in a radar cross section of the ground at 1 km of about -16 dBsm (i.e., 1/40 m^2). At a range of 0.50 km, the illuminated patch is smaller, so that with a σ^o of -20 dB, the radar cross section is about -8 dB below a square meter.

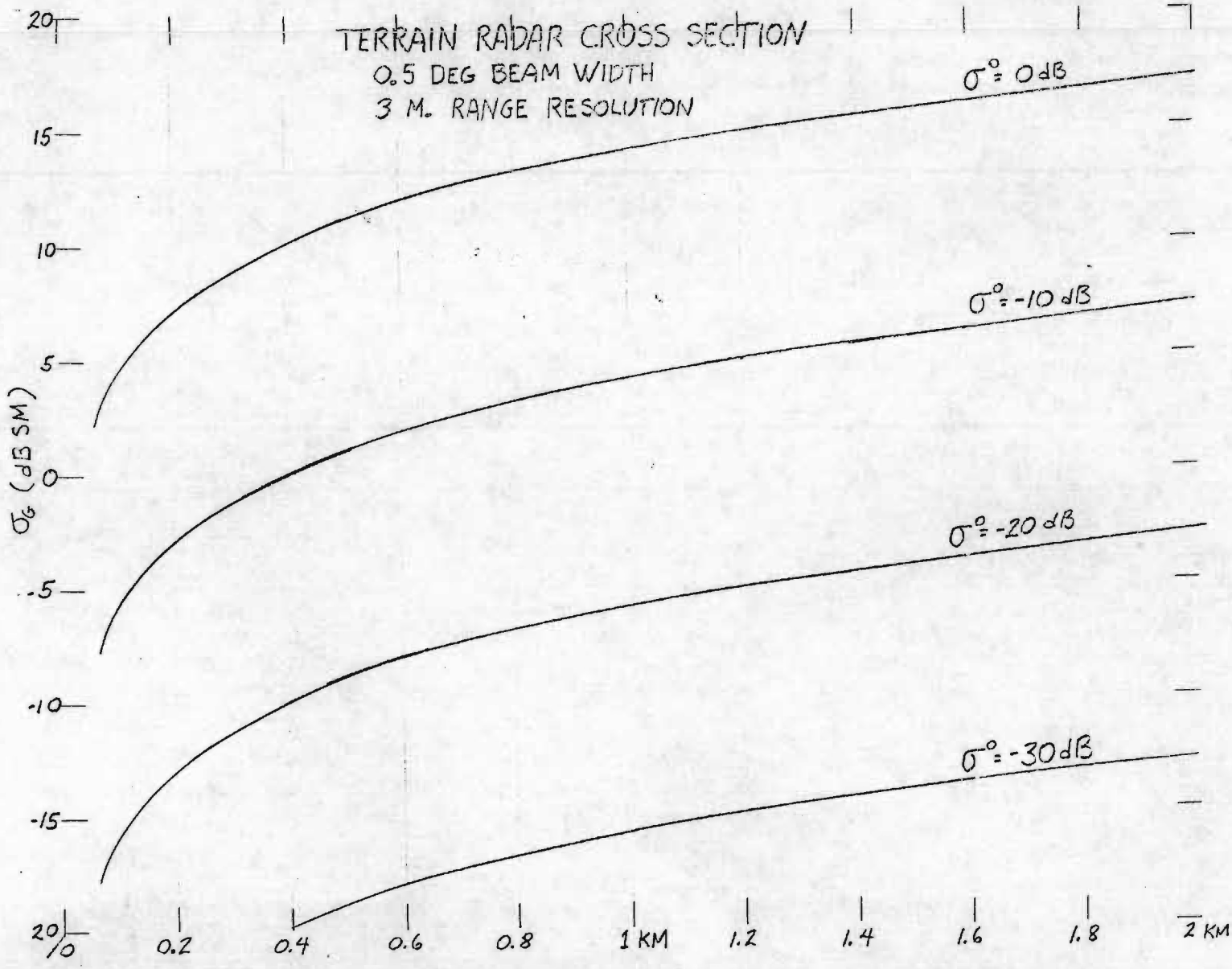

Figure 31. Terrain radar cross section.

The ratio of the ground cross section (Figure 31) to the cross section of rain (Figure 29) is an indication of the probability of detecting the terrain in rain. Figure 32 depicts terrain-to-rain backscatter ratio as a function of range for 25 mm/hr rain and several different values of terrain reflectivity. At a range of 1 km, the radar cross section of 25 mm/hr rain is about equal to the radar cross section of a -23 dB reflectivity terrain. Given a requirement for a terrain-to-rain backscatter ratio of at least 10 dB as a detection threshold, terrain having a reflectivity of -13 dB is detectable at a range 1 km, and terrain having a reflectivity of -10 dB is detectable at a range of 2 km.

A 95-GHz radar operating in a rain as heavy as 25 mm/hr will not detect smooth terrain ($\sigma^o < -20$ dB) until the range closes to less than about 200 meters. This radar should be used to look for corner reflectors or for big scatterers that must be avoided; if nothing is visible, the area can be assumed to be clear of obstacles.

3.2 DUAL FREQUENCY ANTENNA

3.2.1 HYBRID DUAL FREQUENCY ANTENNA

For helicopter use, integration of a MMW radar with the present X-band weather radar will require a dual-frequency antenna. The present X-band slotted waveguide array can be modified to include a 95-GHz parabolic antenna. The concept is shown in Figure 33. A small hole is needed in the center of the X-band array so that a 95-GHz feed can be brought through it. A paraboloid of plastic or foam with a surface of closely spaced, very short wire segments is mounted in front of the feed. The wire segments are short, so they are resonant at 95 GHz and much too short to be reflecting at X-band. Thus, the X-band energy will propagate through the surface with little interaction. This paraboloid is dichroic, i.e., frequency selective, resonant at one frequency and transparent at the other frequency. A polarization twist surface that is also dichroic is placed between the slotted array and the dichroic parabola. The polarization twist surface is formed by a two-layer wire grid. The wires are oriented at 45° to the wires on the parabola; the front side wires are oriented at 90° to the back side wires.

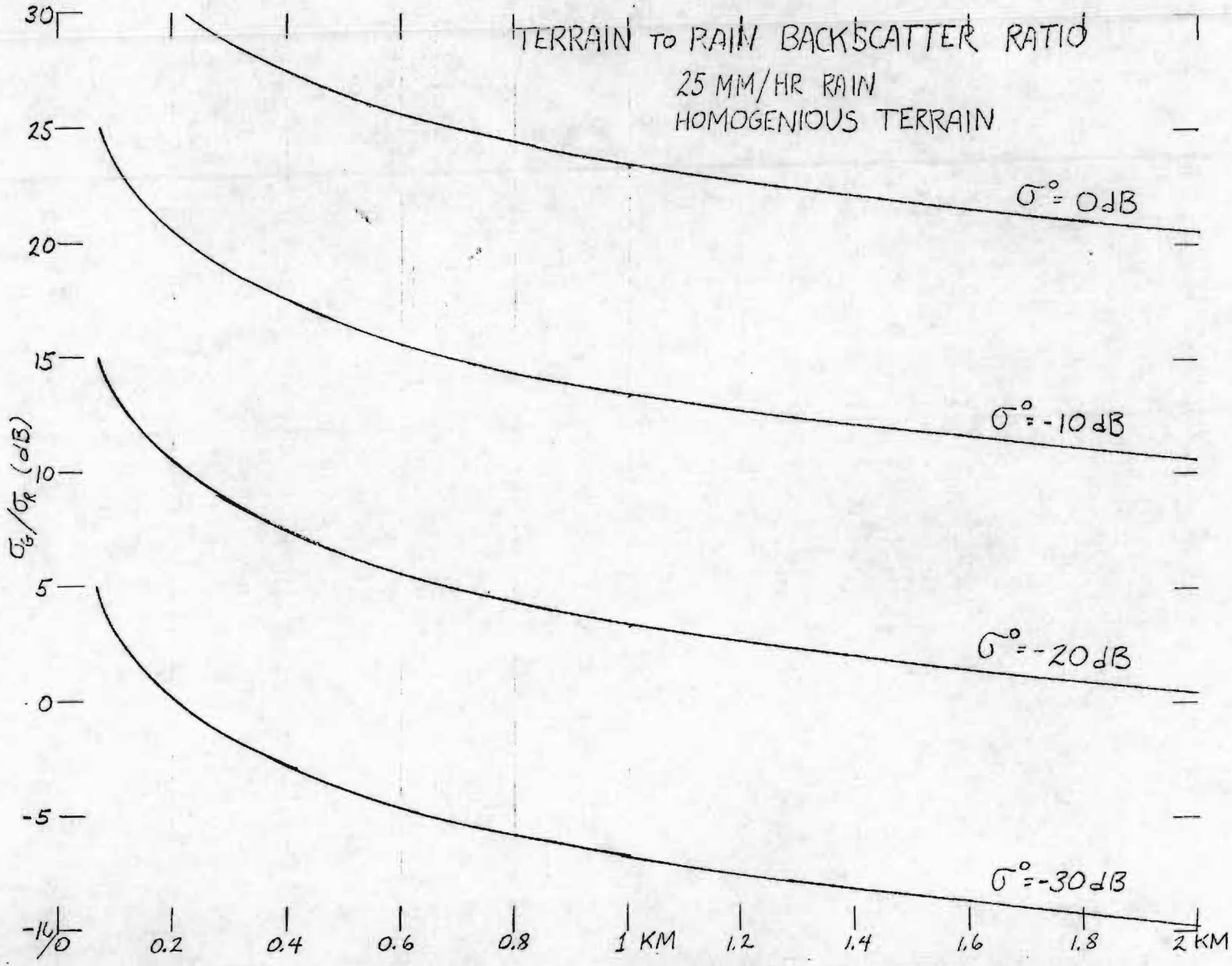

Figure 22. Terrain to rain backscatter ratio

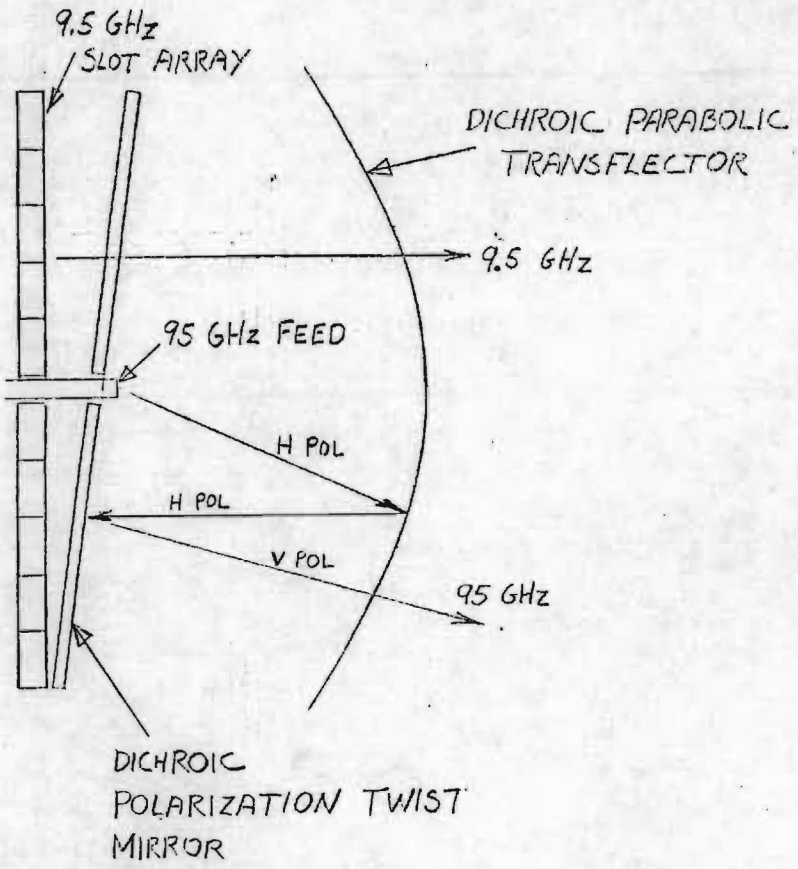

Figure 33. Hybrid dual frequency antenna.

The transmitted MMW energy is radiated by the feed horizontally polarized and is then reflected and collimated by the parabolic surface. This horizontally polarized plane wave is reflected and twisted to vertical polarization by the flat polarization twist grid and then propagates without interference through the horizontal wires of the parabola. As with a mirror, beam scan angle is twice the reflector scan angle. The advantages of this configuration are a low inertia scanner and no RF rotary joints. Since the wires in the parabola and the polarization twist grid are approximately 0.5 wavelengths long at 95 GHz, they are about 0.05 wavelengths at 9.5 GHz and, therefore, much too short to affect the X-band radiation.

3.2.2 PARABOLIC DUAL FREQUENCY ANTENNA

The dichroic antenna concept can be extended to replace the X-band slotted waveguide array. If the front parabola were made of continuous wires, i.e., not dichroic and not resonant at 95 GHz, then the X-band energy would also bounce off the parabola. So if a dual-frequency feed were used to feed the parabolic wire grid (horizontally polarized at both X-band and at 95 GHz), then the X-band energy would be reflected and focused by the parabola, pass through the dichroic polarization twist surface that is resonant at 95 GHz, and be reflected and twisted in polarization by a stationary 9.5 GHz polarization twist grid. The vertically polarized X-band energy would then pass freely through the 95 GHz grid and horizontally polarized parabola. This concept is shown in Figure 34. At MMW frequencies, this antenna would function like the other dichroic antenna. The higher frequencies would be reflected by the horizontal wire grid parabola, be twisted by the mirror, and come back through the parabola again. In this case, the parabolic surface is used to focus both the millimeter wave and the X-band frequencies without the need for a slotted waveguide array.

3.2.3 EXPERIMENTAL ANTENNA

Figures 35 is a photograph of an experimental dichroic polarization twist mirror scan antenna that was built in 1973. In this case, the frequencies were X-band and L-band (10:1 frequency ratio). The parabola is resonant at X-band and the array of spirals operates at L-band. The parabola is 10 inches in diameter.

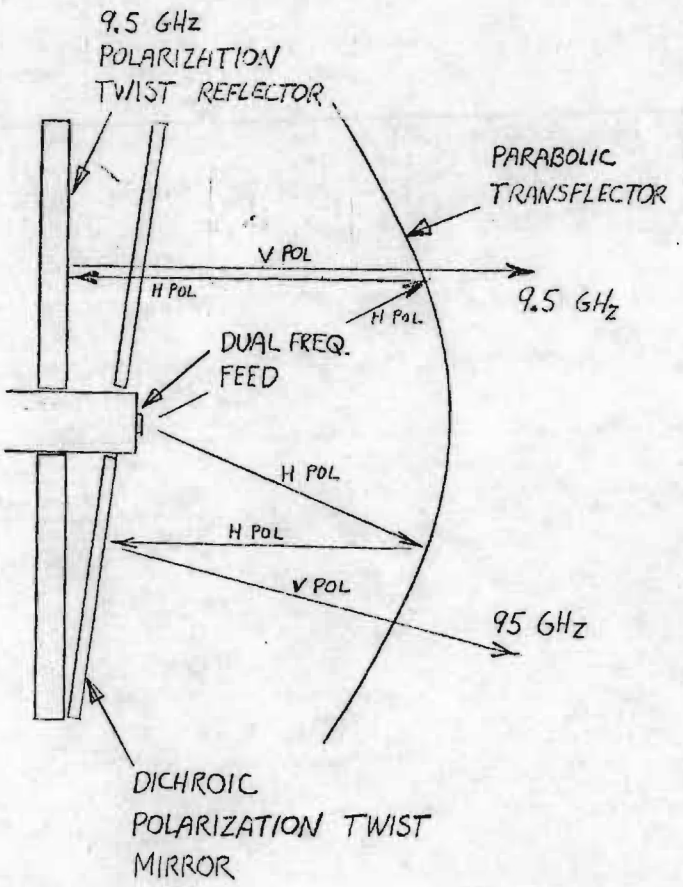

Figure 34. Parabolic dual frequency antenna.

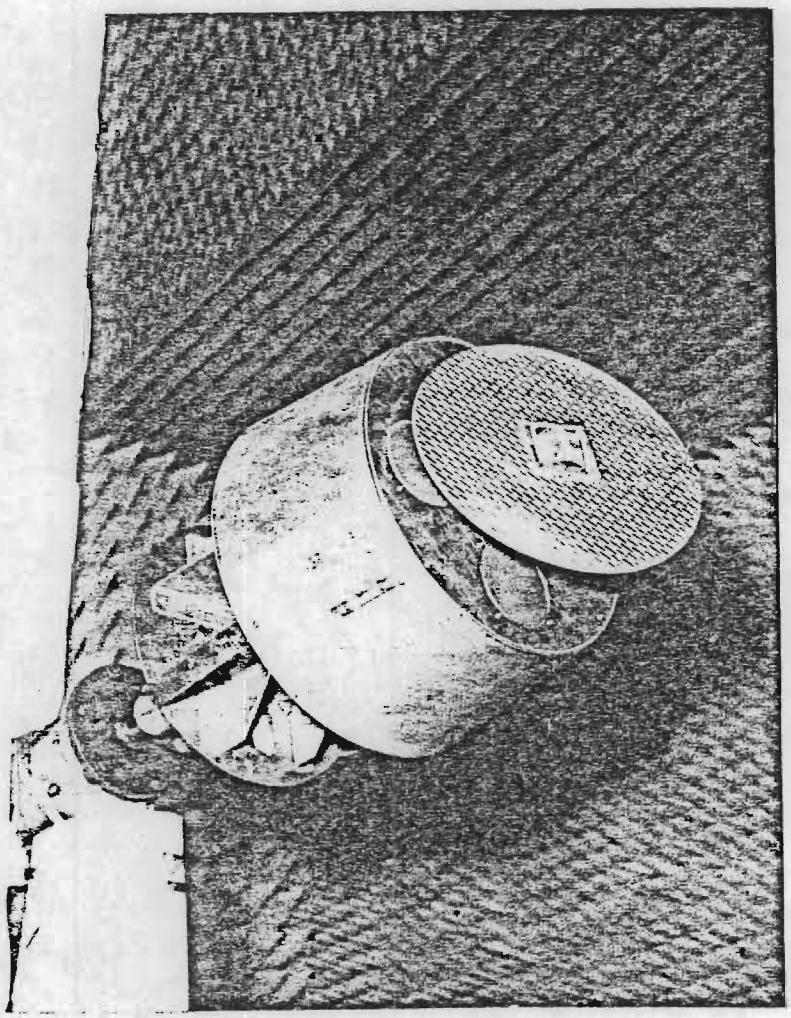

Figure 35. Experimental Dichroic Polarization Twist Mirror Scan Antenna

The X-band antenna pattern for this antenna is shown in Figure 36. The pattern shows a well behaved beam with sidelobes approaching -18 dB. An 18-inch antenna built the same way can be expected to exhibit sidelobes better than 20 dB. At least one 30-inch version of this antenna had sidelobes better than 25 dB. Polarization twist antennas have also been built at 95 GHz; however, these antennas have been 4 to 7 inches in diameter. The experimental 10-inch X-band antenna would scale to about 1-inch at 95 GHz, i.e., about 8 wavelengths in diameter. A larger antenna will have lower sidelobes and a narrower beamwidth. Based on available evidence, an 18-inch, 95 GHz dichroic polarization twist mirror scan antenna is certainly within the state-of-the-art.

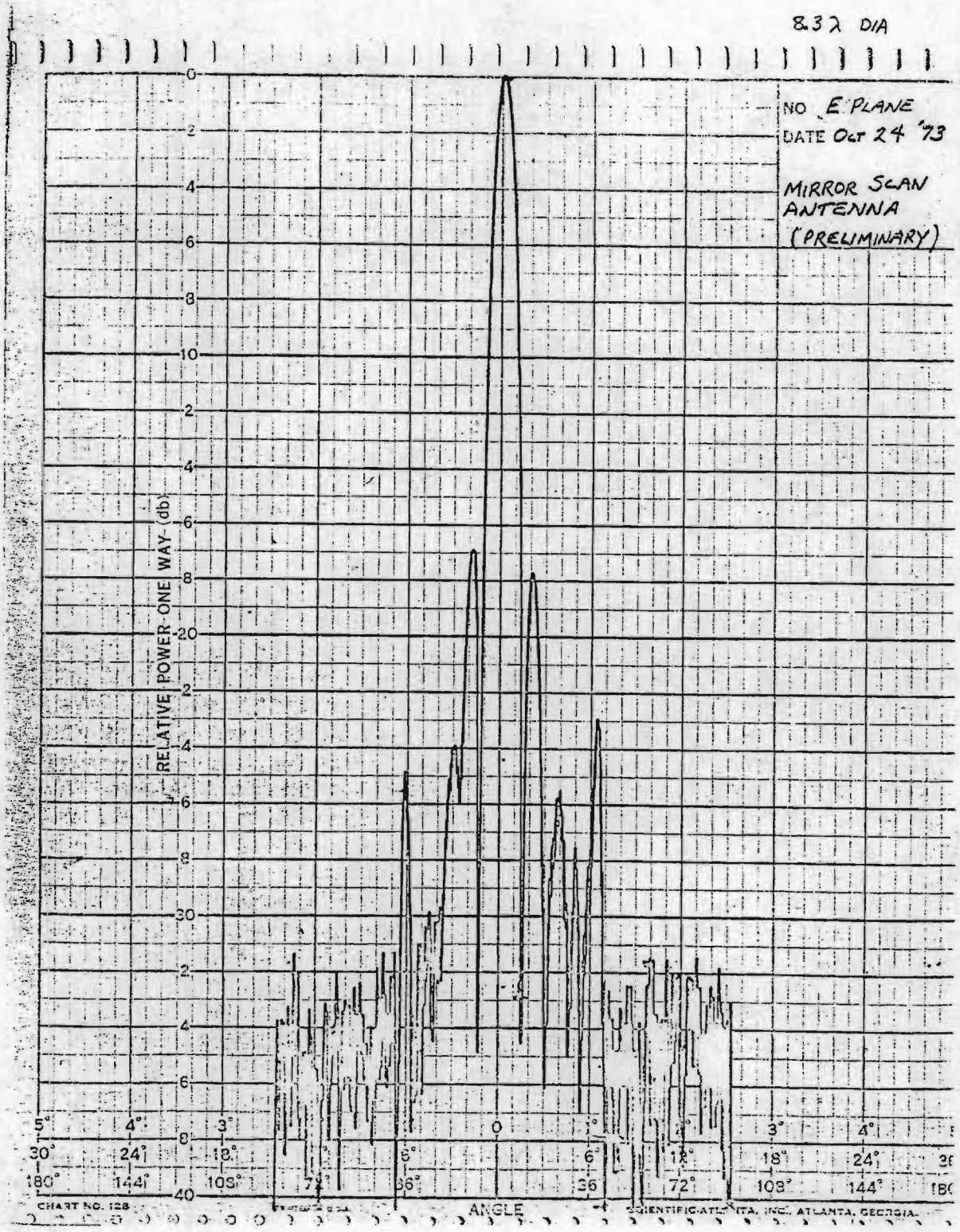

Figure 36. Mirror scan antenna pattern.

SECTION 4
CONCLUSIONS AND RECOMMENDATIONS

The results of analyses performed in the rotary wing antenna study show that sufficient control of the elevation pattern can be obtained with an antenna that is relatively simple in cross section and compatible with basic helicopter wing designs. The dielectric materials in the wing were not included in the simulations; these will affect detailed antenna design, but are not expected to change achievable elevation pattern performance. In fact, antenna performance may not be appreciably affected by the wing, since the bulk of that part of the wing through which the antenna must look consists of the low dielectric (about 1.1) nomex core. Final antenna design, however, must be verified with the antenna in the wing.

This analytical study should be followed by an empirical rotary wing antenna development effort. Since only the elevation pattern will be critically affected by the wing, only a short wing section will be required for testing. More than one wing section may be needed if the wing cross section changes appreciably over the antenna length. Extra core material will be needed to replace material removed for the purpose of inserting the trial antenna configurations. During this empirical process, computer simulation can provide guidance for modifying the conducting parts of the antenna to compensate for the effects of the wing materials.

The results of the dual frequency radar study show that a forward looking millimeter wave radar is capable of providing adequate resolution radar data. The performance of a millimeter wave radar, however, is severely limited in 25 mm/hr rain, but may be satisfactory in 10 mm/hr rain.

REFERENCES

1. E. H. Newman, "A User's Manual For: Electromagnetic Surface Patch (ESP) Code," The Ohio State University Electroscience Laboratory Technical Report 713402-1, July 1981.

2. V. H. Rumsey, "The Reaction Concept in Electromagnetic Theory," Physical Review, June 15, 1954.

3. "Microwave Intervisibility System (MIS) Phase I - Concept Formulation," by F. R. Williamson, S. P. Zehner, E. F. Knott, J. A. Scheer, S. D. Hunt, and L. C. Bomar, June 1981

4. "Analysis of Radar Rain Return at Frequencies 9.375, 35, 70 and 95 GHz," by N. C. Currie, F. B. Dyer, and R. D. Hayes, February 1975